Effect of Al_2O_3 / Water Nanofluid Concentration on Heat Transfer and Fluid Flow Characteristics in U Type Flow Cross Flow Compact Heat Exchanger

A

Dissertation

Submitted in partial fulfillment of the requirements for the award of degree of

Master of Engineering (M.E.)

In

Thermal Engineering

Submitted by

Sandeep Kumar

(ROLL NO. 801283023)

UNDER THE GUIDANCE OF

Dr. D Gangacharyulu
(Professor)
(CHED)

Mr. Sumeet Sharma
(Associate Professor)
(MED)

DEPARTMENT OF MECHANICAL ENGINEERING

THAPAR UNIVERSITY, PATIALA – 147004

JULY 2014

CERTIFICATE

I hereby declare that the Dissertation **"Effect of Al_2O_3 /water nanofluid concentration on heat transfer and fluid flow characteristics in U type flow cross flow Compact Heat Exchanger"**. is an authentic record of my study carried out as requirements for the award of the degree of **Master of Engineering** in **Thermal Engineering** at **Thapar University, Patiala** under the supervision of **Mr. Sumeet Sharma**, Associate Professor, Mechanical Engineering Department, and **Dr. D Gangacharyulu**, Professor, Chemical Engineering Department, Thapar University, Patiala during July 2012 to July 2014. The matter embodied in this report has not been submitted in partial or full to any other university or institute for the award of any degree.

Sandeep

Date: 16-07-2014

Sandeep Kumar
(801283023)

It is certified that the above statement made by the student is correct to the best of my/our knowledge and belief.

21/7/14

(D. Gangacharyulu)
Department of chemical Engineering
Thapar University, Patiala - 147004

(Sumeet Sharma)
Department of Mechanical Engineering
Thapar University, Patiala - 147004

Countersigned by

(Ajay Batish)
Professor & Head
Mechanical Engineering Department
Thapar University, Patiala - 147004

(S.K Mohapatra)
Sr. Professor
Mechanical Engineering Department
Dean of Academic Affairs
Thapar University, Patiala - 147004

Dedicated to My parents

Rakesh Kumar

Avtar Kaur

&

Brother Sumit Kumar

ACKNOWLEDGEMENT

I am extremely fortunate to be involved in an exciting and challenging research project like **"Effect of Al_2O_3 /water nanofluid concentration on heat transfer and fluid flow characteristics in U type flow cross flow Compact Heat Exchanger"**. It has enriched my life, giving me an opportunity to work in a new environment of heat transfer and Nanofluids. This project increased my thinking and understanding capability and after the completion of this project, I experience the feeling of achievement and satisfaction.

I would like to express my greatest gratitude and respect to my supervisors **Mr. Sumeet Sharma, Associate Professor,** Mechanical Engineering Department, and **Dr. D Gangacharyulu, Professor,** Chemical Engineering Department**,** for their excellent guidance, valuable suggestions and endless support. They have not only been a wonderful supervisors but also genuine persons. I consider myself extremely lucky to be able to work under guidance of such dynamic personalities.

I also express my special thanks to **Dr. Ajay Batish,** Professor and Head, Mechanical Engineering Department, and **Dr. S.K Mohapatra,** Sr. Professor, Mechanical Engineering Department, and Dean Academic Affair, Thapar University Patiala providing me opportunity to conduct this work and bring it out in present form.

Last but not the least; I want to convey my heartiest gratitude to my parents and my friends for their immeasurable love, support and encouragement.

(Sandeep Kumar)

ABSTRACT

Heat transfer and fluid flow characteristics of U type flow cross flow compact heat exchanger was measured experimentally under laminar flow conditions. Al_2O_3 nanoparticles were used to prepare nanofluids at 0.1% by vol. and 0.2% by vol. concentration in distilled water. Flow rate in heat exchanger was varied from 25 liters / hour to 40 liters / hour. Air makes cross flow through the tubes, whose flow rate was varied from 241.92 m^3 / hour to 728.35 m^3 / hour. Cross flow heat exchanger consisted of 28 flat brass tubes in two rows with copper multi louvered fins. In heat exchanger, working fluid entered in tubes at inlet temperature values of 45°C, 50°C, and 55°C. Experimental results showed that increase in nanofluid flow rate and concentration with temperature, heat transfer coefficient was increased by 16.38% to 18.51%. Effectiveness of cross flow heat exchanger was increased from 68.52% to 72.56%, and 74.21% for 0.1% by vol., and 0.2% vol. concentration respectively. Friction factor value increased to 11.11% and 25.56% at 45°C temperature for 0.1% by vol., and 0.2% vol. concentration respectively. But as the flow rate of fluid at tubes side increased the value of friction factor decreased by 60%.

TABLE OF CONTENTS

LIST OF FIGURES

LIST OF TABLES

Nomenclature

A_t : total heat transfer surface area, m^2

A_o : free flow areas of the exchanger, or Cross section area of exchanger, m^2

A_f : surface area of fin exposed to heat transfer, m^2

A_{fr} : air side frontal area on one side of the exchanger, m^2

A_{nft} : non fin area, m^2

$A_{c,t}$: cross section area of tube, m^2

A_w : Airways

T_t : tube thickness

T_w : tube width

T_l : tube length for small cross section, m

$T_{t,l}$: total tube length in core dimension, m

T_s : tube sheet thickness, m

F_t : fin thickness, m

F_l : fin length, m

F_w : fin width, m

$F_{t,l}$: total fin length, m

N_t : number of tubes one side

N_f : number of fins in between two tube.

N_s : total number of fins one side

A : tube spacing, m

a : half fin length for small cross section = (tube spacing)/2, m

B : fin spacing, m

b : half of tube thickness for small cross section = (fin spacing)/2, m

W : fluid flow (air) length, m

C_f : circumference of fin exposed to heat transfer, m.

C_p : specific heat of fluid at constant pressure, J/kg ^{0}C.

D_h : hydraulic diameter of flow passage, m

f : friction factor, dimensionless

G : mass velocity, kg/m^2 s

C : heat capacity rate

H : total water flow length, m

h : heat transfer coefficient, W/m^2 ^{0}C

J : Colburn factor, dimensionless

K : fluid thermal conductivity, W/m ^{0}C

k_f : thermal conductivity of fin material, W/m ^{0}C

l : fin length for heat conduction from primary to the midpoint between plates, m

L : non-fluid flow length, m

LPH : Liters per hour.

f_p : fin parameter, m^{-1}

P : pressure, Pa

Pr : Prandtl number, dimensionless

Nu : nusselt number

Re : Reynolds number based on hydraulic diameter, dimensionless

r_h : flow passage hydraulic radius, m

T : fluid temperature, ^{0}C

U : overall heat transfer coefficient, W/m^2 ^{0}C.

V : volume, m^3.

v : velocity, m/s.

m : fluid mass flow rate, kg/s.

R_c : fouling resistance, $W/m^2\ ^0C$.

R_t : tube wall resistance, $W/m^2\ ^0C$.

R_h : fouling resistance, $W/m^2\ ^0C$.

α : ratio of total heat transfer area of one side to its volume, m^2/m^3.

ρ : density, kg/m^3.

δ : thickness of fin, m.

μ : fluid dynamic viscosity, Pa.s.

σ : ratio of free flow area to frontal area, dimensionless.

ϕ : diameter, m.

φ : volume fraction.

ε : thermal conductivity enhancement.

η_f : fin efficiency

η_0 : overall efficiency

ξ : heat exchanger effectiveness.

Subscripts

a : air

b : bulk

c : cold fluid side

h : hot fluid side

w : water

1 : inlet condition

2 : outlet condition.

CHAPTER-1

Introduction to Cross Flow Heat Exchanger and Nanofluids

1.1 Introduction

Devices that are used for transferring the thermal energy between fluid and solid surface or between two fluids or more than two fluids in thermal contact when they are at different temperature are called heat exchangers. Heat exchangers involves only heating or cooling, evaporation or condensation of single and multi component of fluid and no externally heat and work interaction. Objective of heat exchanger is to recover or reject heat from a system. Flow of heat is function of heat transfer area, temperature difference and conductive or convective properties of fluid. Convective heat transfer between fluid and surface is given by Newton's law of cooling which is given by equation

$$Q_C = h*A* (T_S-T_f) \quad (1.1)$$

Where 'h' is 'convective heat transfer coefficient in (W/m^2K)', A is heat transfer surface area in (m^2), T_S is surface temperature in (K) and T_f is fluids temperature in (K).

1.2 Classification of heat exchanger

Depending upon type of application heat exchangers are classified in various categories [17].

(1) According to transfer process.
(2) According to flow arrangement.
(3) According to surface compactness.
(4) According to pass arrangement.
(5) According to construction.
(6) According to phase of fluid.
(7) According to heat transfer mechanisms.

Classification of heat exchangers in brief are given with the help of chart

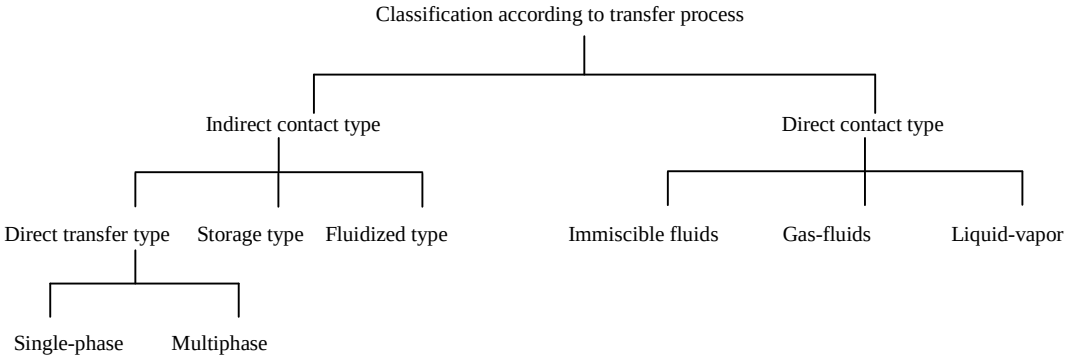

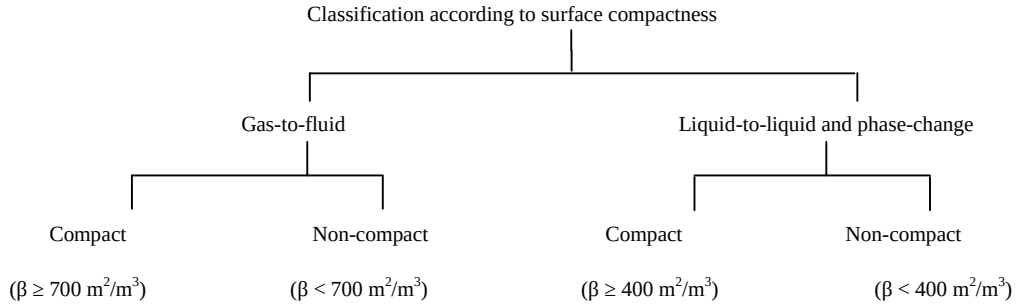

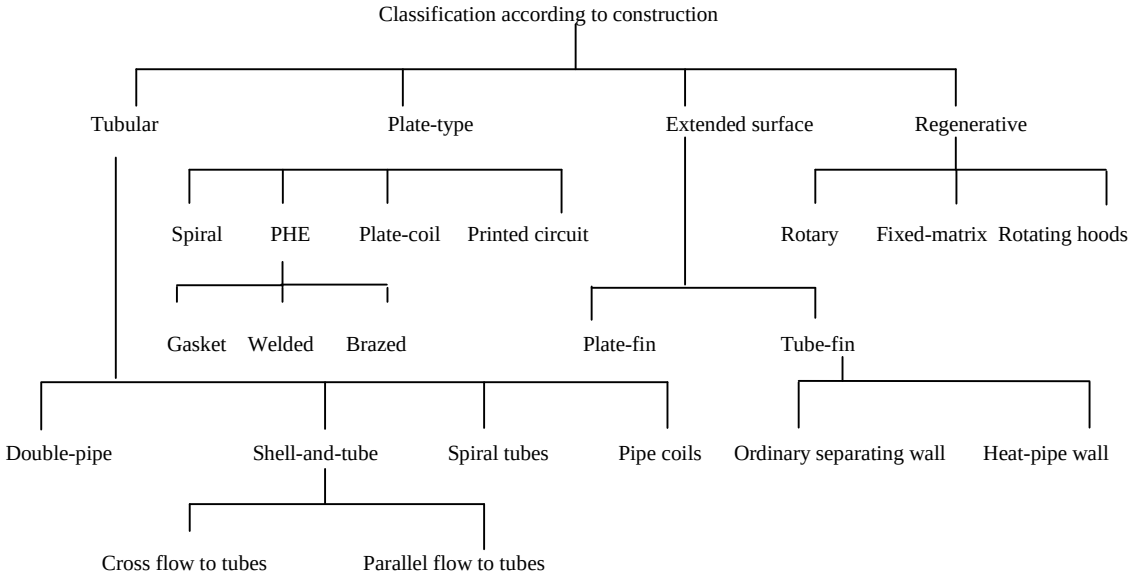

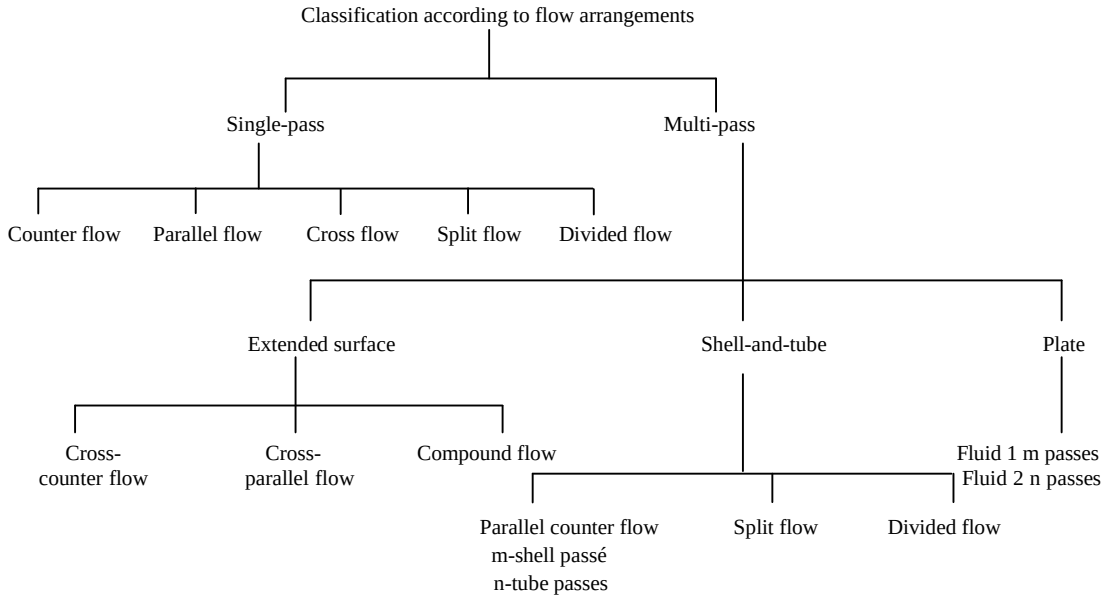

Fig. 1.1: Classification of heat exchangers [16]

For any heat exchanger main requirement is its heat load and how fast and effectively heat exchanger does heat transfer. To increase the heat transfer rate we have to increase the (h*A) value and this can be done by either increase surface area or increase heat transfer coefficient or increase both, but heat transfer coefficient of fluid cannot be change and for constant heat transfer coefficient we can increase either area or temperature. Temperature difference increment has various limits, for example to supply hot fluid at high temperature and cold fluid at lower temperature extra work has to be done. Further increase in temperature lead to thermal stress in material of heat exchanger which leads to deformation of material and decrease the lifecycle of heat exchanger. To avoid this problem surface area of exchanger is increased and this need gives rise to birth of compact heat exchanger.

Compact heat exchanger are distinguished from other class of heat exchanger because of large surface area per unit volume which results in reduce in weight, energy requirement, space and cost. Surface area is $\geq 700\ m^2/m^3$for liquid to gas, and $\geq 400\ m^2/m^3$for liquid to liquid heat exchanges respectively with hydraulic diameter is $\leq$ 6mm. It consist of core matrix for distribution of fluid and provide large heat transfer surface area. Flow distribution part consists of header, manifolds tank, pipes, outlet and inlet nozzle seals etc.

1.3 Important operating and design consideration

Important operating and design consideration for compact heat exchanger are listed below.

(1) High compactness led to large frontal area and having short flow length.
(2) Temperature and pressure is limited as compare to shell tube heat exchanger.
(3) At least one fluid having low convective heat transfer coefficient i.e. gas.
(4) Pressure drop and pumping power is very important for heat transfer.
(5) The hydraulic diameter of tubes is very small so fluid is free from dust and debris.
(6) Compact heat exchangers are not operating in high fouling application.

1.4 Tube fin compact heat exchange

These are conventional type of heat exchanger means heat is transferred between two fluids first by conduction between fluid and tube surface and, by convection from tube surface to other fluid passed over extended surface by forced draft fan or by induced draft fan. In liquid to gas heat exchangers convective heat transfer coefficient on liquid side is much greater than the gas side and surface area on gas side is much greater than liquid side to balance the thermal conductance (h*A). For lager surface area fins are used at gas side attached to tube. Tubes are of different types having different cross section area like flat rectangular, elliptical, circular, and round rectangular. Tube fin heat exchanger can withstand high operating pressure on tube side but for high temperature it has certain limitations like type of bonding, material used, material thickness, conductivity of material etc.

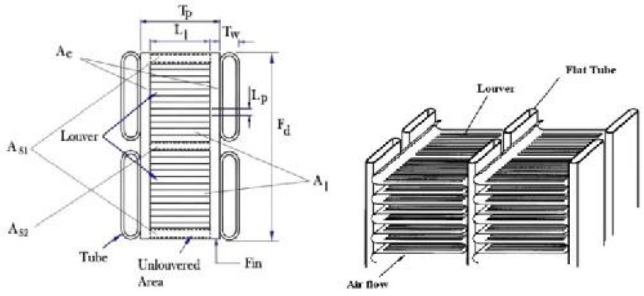

(a) (b)

Fig. 1.2: Tube and louvered fin arrangement [17]

1.4.1 Tube fin heat exchanger classification

Tube fin heat exchangers are classified according to type of fin used and arrangement of fin.

(1) Individually finned tube
   (a) Plain circular
   (b) Helical
   (c) Annular fin geometries like spine, studded, slotted and wire loop fins.
(2) Array of tubes in continuous fin and fin may be plain, wavy, louvered type.
(3) Longitudinal fin on individual tube.
(4) Fins on inside of tube are of two types a) integral fins b) internally attached fins.

1.4.2 Application of tube fin heat exchanger

Tube fin heat exchangers are used in many industrial applications like evaporator and condenser in refrigeration and air conditioning units. Tube fin are also used in internal combustion engines for water and oil cooling through radiators, pre-heaters, and after-coolers. Automotive condenser and evaporator are also used in automotive industry.

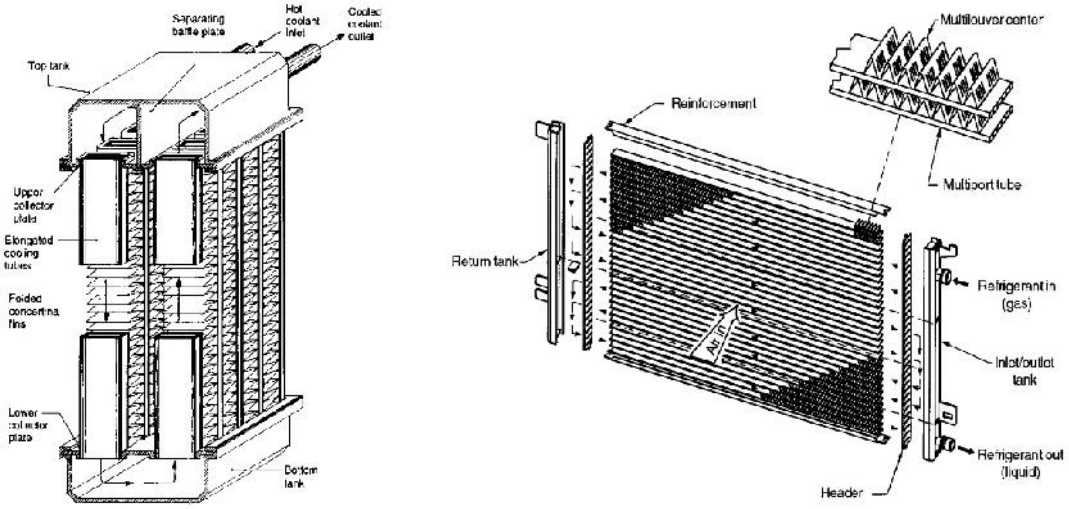

(a) (b)

Fig. 1.3: Cross flow heat exchanger (a) automotive radiator (b) Refrigerator [16].

1.4.3 Radiator

Radiators are one of type of tube fin liquid to gas heat exchanger and important component of automotive vehicles. Radiators have flat brass tube present in one row or multi row with plain or louvered type copper fins soldered together in a unit to form radiator's core matrix. Aluminum radiators have flat tube with corrugated fins brazed together in single unit. Louvered fins are mostly preferred because of low fin density with same heat transfer area with same thermal performance over plain or non-louvered fins. Fin density is ranging from 10-25 FPI and surface area density is 900-1650 m^2/m^3 [17].

The present day global economics produce more efficient equipment at low cost without sacrificing the original performance. Energy, material saving and space consideration led to produce compact type heat exchanger with improved thermal performance with minimum operating cost. To improve the thermal performance or heat transfer performance various methods are used such as compact surfaces, enhanced surfaces etc. There are two types of technique used in this heat transfer enhancement a) Passive method. b) Active method.

Active technique: (a) Stirring of fluid. (b) Surface vibration. (c) Fluid vibration.

Passive technique: (a) Treated surface (b) rough surface (c) Extended surface (d) Swirl flow device (e) Additive for liquids

1.5 Introduction to Nanofluids

New technique is recently in trend i.e. use of solid particle in suspension with liquid to enhance the thermo-physical properties of fluid flowing in heat exchanger. It increases the thermal performance and effectiveness of exchanger. These particles are of 1-100 nano meter in size dispersed in liquid to form meta-stable Fluid called Nanofluid. Nanofluids are panacea for thermal equipments. Recently it has been recognized as an opportunity to widen the next-generation's smart coolants for mechanically advanced devices that have shifted the paradigm to miniaturization but without compromising in working efficiency, power but these device results in more heat generation. Designing energy efficient and enhancement

methods in heat transfer rate are one of the most important and challenging area in various industrial applications. To maintain the desired performance cooling is essential and for safe operation of wide variety of equipments and devices such as higher power engines, fuel cell, microelectronic devices (operated at high speed), super conducting magnets, ultrahigh-heat flux optical devices, x-rays machines, high-powered lasers, etc. Sometimes heat load exceeds 2000 W/cm2 [1] caused by compact size and high heat production rate. But the working fluids such as water, ethylene glycol, and oil etc. have poor heat transfer properties. Therefore there is a strong demand to develop the advanced heat transfer fluids with higher heat transfer properties. Development of high energy efficient heat transfer devices thermo fluid properties play very important role. To obtain higher heat transfer properties, various theoretical and experimental studies have been done. Maxwell (1873) did great effort by dispersing millimeter or micrometer size particles in liquids. However the major problem was settling down of large particles in suspension [2]. The key idea was that the very high thermal conductivity of solid particles which can be hundreds and even thousand times greater than that of the conventional heat-transfer fluids such as ethylene glycol and water shown in (Table 1.1). Keeping in mind Maxwell's concept, a new innovative concept of Nanofluids has come in to existence.

The term Nanofluid is coined by "Choi" in 1995 at the Argonne national Laboratory (ANL) [3]. Nanofluids are solid liquid composite materials consisting of solid nanoparticles typically of size (1-100) nm suspended in liquid. Suspended nanoparticles in conventional fluid are called Nanofluids. Nanofluids greatly enhance thermal properties hence thermal engineers take great interest in this new concept. Modern nanotechnology can produce metallic or non-metallic particles and carbon Nanotube of nanometer dimensions suspended in base fluid in small amount extensively increase thermal conductivity [4-6].

Nanomaterials have unique mechanical, optical, electrical, magnetic, and thermal properties. Nanofluids are engineered by suspending nanopartic1es with average sizes below 100 nm in traditional heat transfer fluids such as water, oil, and ethylene glycol. The purpose of nanofluids is to achieve the highest possible thermal properties at the smallest possible concentrations [1]. Thermal conductivity of metallic liquid is much greater than that of non-metallic liquids as shown in (Table 1.1**).** Therefore the thermal conductivity of fluids that

contain suspended solid metallic particles is significantly higher than those of conventional heat transfer fluids [7]. Various enhancement mechanisms of thermal conductivity are studied that contribute in thermal conductivity [8-9](1) Brownian motion of nanoparticles.(2) Layering liquid molecules at liquid/particle interface.(3) Ballistic nature of heat transport. (4) Nanopartic1e clustering

Table 1.1: Thermal conductivity of various materials [14]

Materials		**Thermal conductivity (W/m.K)[a]**
Metallic solids	Silver	429
	Copper	401
	Aluminium	237
Non-metallic solids	Diamond	3300
	Carbon nanotube	3000
	Silicon	148
	Alumina(Al_2O_3)	40
Metallic liquids	Sodium at 644 K	72.3
Non-metallic liquids	Water	0.613
	Ethylene glycol	0.253
	Engine oil	0.145

a At 300 K unless otherwise noted

1.5.1 Importance of nanofluid in thermal engineering

Nanofluids enhance heat transfer as we know that the size of heat transfer devices is getting scaled down gradually, so it necessitates the better cooling processes. Due to scaling down and high operating speed of devices such as micro-electro mechanical systems [MEMS], temperature increases to high limits which become a constriction for devices to operate at high power. Fluids used for cooling (water, oil, etc.) have poor thermal conductivity which leads to equipment limitation, reduced thermal and processing efficiency. Nanofluids recently have made its place in this advanced cooling mechanism and enhanced thermal

conductivity of fluids. Enhancement in thermal properties depends on volume fraction of nanoparticles as shown in (fig 1.1). With small particles concentration of nanoparticles we can increase heat transfer rate in thermal systems and can meet the cooling needs of thermal systems. Nanoparticle size play a very important role in enhancement of thermal conductivity as particle size below 50 nm the enhancement in thermal conductivity increased by 40% when 3% (v/v) CuO particles are used in ethylene glycol [11]. Therefore Nanoparticles enhanced the thermal conductivity and this enhancement makes lighter size heat exchanger with slow flow velocity, leading in reduced pump work attributable to less erosion in pipes and other components.

Enhance heat transfer rate because nanoparticles have large surface area to volume ratio. A continues heat exchange between nanoparticles and base fluid through convection mechanism depending base fluid temperature and velocity of nanoparticle relative to base fluid [12] increase the heat transfer rate. Role of Brownian movement in heat transfer is very important in case of nanofluids. Heat transfer takes place when collision between particles occurs due to Brownian motion which depends on temperature and viscosity of base fluid, nanoparticle size. As temperature of base fluid increases its viscosity decreases and Brownian motion increases hence conductivity increases. The random motion of particles in base fluid is depend on particle size. Decrease in particle size leads to large motion and convection heat transfer phenomenon become dominant. [13].

1.5.2 Importance of Nano size

Maxwell [2] adds micro size solid particles in fluids to enhance the thermal conductivity. The major problem that arose was that these micro particles settled down rapidly in base fluid. Settled particles formed a sediment layer at low flow velocity and decrease the thermal conductivity enhancement. These particles agglomerate at low flow circulation in micro channels and caused clogging problem. Faster cooling occur (because of stable suspension) in heat transfer fluid. Nano size particles have very good thermal properties. Nanoparticles have high surface to volume ratio. Main properties which tell the difference between micro size and nano size particle is shown in table (1.2) give some idea why nano size is so important.

Table 1.2: Comparison of Micro size and Nanosize particle [1].

Properties	**Micro particles**	**Nanoparticles**
Stability	Settle	Kinetically stable (long lived in suspension)
Surface/volume ratio	1	1000 times larger than micro particles.
Conductivity[0]	Low	High
Erosion & clogging	Yes	No
Pump power	High	Low

[0]At the same operating conditions.

1.5.3 Materials for Nanoparticle

Table 1.3: Different material for nanoparticle [15]

Material	Form	Thermal conductivity (W/mK)
Carbon	Nanotube Diamond Graphite	1800-6600 2300 110-190
Metallic solids	Silver Copper Nickel	429 401 237
Non metallic	Silicone	148
Metallic liquids	Aluminium Sodium at 644K	40 72.3
Others	Water Ethylene Engine oil	0.613 0.253 0.145

1.5.4 Types of host Fluid

- **Metallic fluids**
  - Sodium
- **Non-metallic fluids**
  - Water
  - Ethylene glycol
  - Oil

1.5.5 Preparation of Nanofluids [1]

Nanoparticles are Metastable in fluids for long time. Nanoparticles preparation is done by two methods:

- The two-step method: This is common and widely used method for preparation of nanofluid. Dry powder of Nanofibers, nanoparticles, is made by different methods (Physical method include Inert-gas condensation (IGC), mechanical grinding. Chemical method includes chemical vapour deposition (CVD), chemical emulsion, thermal spray pyrolysis) and then disperse into base fluid with the help of ultra- Sonication, intensive magnetic force agitation, surfactants.
- The single-step method: In this process nanoparticles simultaneously make and disperse directly into base fluid. This is the advance method from two-step preparation. To minimise the problem of agglomerate one step method is used in which physical vapour condensation of metal and metal oxide. One-step physical method cannot produce nanoparticles at large scale and cost is also high. One-step Chemical method is developing rapidly.

1.5.6 Advantage of Nanofluids

- Better stability as compared to micro size, mili-sized particles.
- High heat conducting capability.
- High surface to volume ratio which provide large area for heat interaction between nanoparticles and base fluid.

- Negligible or small amount of pressure drop required less pump work because of small particle size and low volume fraction.
- No erosion and clogging in device channels hence miniaturization is possible.
- Adjustable thermal conductivity by different volume fraction in base fluid.

1.5.7 Application of nanofluids [1]

- **Cooling applications:** "High intensity x-ray generate tremendous amount of heat (2000-3000W/cm2) as it bounce off minor which should be feasible by nanofluid technology".
- **Vehicles cooling:** Nanofluids not only used as engine oil and coolant but also in lubricant, gear oil, and, transmission fluid.
- **Transformer cooling:** "The power generation industry is interested in transformer cooling application of nanofluids for reducing transformer size and weight. The increased thermal transport of transformer oils translates into either reduction in the size of new transformers at the same level of power transmitted or an increase in the performance of existing transformers".
- **Defence applications:** "Heat transfer fluids. Nanofluids also provide advanced cooling technology for military vehicles, submarines, and high-power laser diodes. A number of military devices and systems, such as high powered military electronics, military vehicle components, radars, and lasers, require high-heat-flux cooling, to the level of thousands of W/cm^2".
- **Other applications:** Other possible areas for the application of nanofluids technology include cooling a new class of super powerful and small computers and other electronic devices for use in military systems, airplanes, or spacecraft as well as for large-scale cooling.

1.5.8 Challenges of nanofluids

- **Long term stability** of nanofluid is a challenging task. They make agglomerate after some time due to strong Van Der Waals forces between molecules when dispersed. To get metastability in nanofluids some physical or chemical treatment is given. For example ultra sonication, surfactants (CTAB, SDBS).
- **High cost** of production of nanoparticles.
- **High nanoparticle** concentration and nanoparticle size pump power is more because viscosity is increased. As Reynolds number of nanofluid increases the pumping power is increases.

1.6 Objective

Heat transfer rate now a day is challenging task for present and upcoming devices. Heat exchanger plays a very important role in the area of heat transfer. New researches in this area of heat transfer target the enhancement of heat exchangers. Various methods are used to increase the heat transfer rate. One of them is use of nanoparticles in heat exchangers to increase the conductive and convective heat transfer rate. Objective of this study

- Study of heat transfer and fluid flow characteristics of Al_2O_3 nanofluids with different concentration of nanoparticles in U-type flow, cross flow compact heat exchanger.

References

[1] Das S.K., S.U.S. Choi, Wenhua Yu and Pradeep T., (2007), Nanofluids: Science and Technology. John Wiley & Sons, Inc. New Jersey.

[2] Maxwell J.C., (1881), "A treaties on electricity and magnetism", 2nd ed., Clarendon Press, Oxford, U.K., Vol 1.

[3] S.U.S. Choi, (1995) "Enhancing thermal conductivity of fluids with nanoparticles, Developments and Applications of Non-Newtonian Flows", FED-vol.231/MD-Vol. 66, 99-105.

[4] Eastman J.A., , S.U.S. Choi, S. Li, W. Yu, L.J12, (2001) "Anomalously increased effective thermal conductivities of ethylene glycol-based nanofluids containing copper nanoparticles" Applied Physics Letters Vol. 78, 718.

[5] H. Xie, H. Lee, W. Youn, M. Choi, (2003) "Nanofluids containing multiwalled carbon nanotubes and their enhanced thermal conductivities" Journal of Applied Physics Vol. 94, 4967.

[6] S.U.S. Choi, Zhang Z.G., W. Yu, Lockwood F.E., Grulke E.A., (2001), "Anomalous thermal conductivity enhancement in nanotube suspensions" Applied Physics Letters Vol. 79, 2252.

[7] Frank P. Incropera, David P. Dewitt, Theodore L. Bergman, Adrienne S. Lavine,(2006), “Fundamentals of heat and mass transfer" John Wiley & Sons. Sixth edition.

[8] Keblinski P., Phillpot S.R., S.U.S. Choi, Eastman J.A., (2002), “Mechanism of heat flow in suspension of nanosized particles” , International Journal of Heat and Mass Transfer Vol. 45, 855-863.

[9] Jang S.P., S.U.S. Choi, (2004), "Role of Brownian motion in the enhanced thermal conductivity of nanofluids", Applied Physics Letters Vol.84, 4316.

[10] Beck Michael P., Yuan Yanhui, Warrier P., Teja A.S., (2009), “The effect of particle size on the thermal conductivity of alumina nanofluids” , J Nanopart Res 11:1129-1136.

[11] Eastman JA, Choi SUS, Li S, (2001), “Anomalously increased effective thermal conductivities of ethylene glycol-based nanofluids containing copper nanoparticles”, Applied Phys Letter Vol. 78, 718-720.

[12] Karthik V., Sahoo S., Pabi S.K., Ghosh S., (2012), “On the phononic and electronic contribution to the enhanced thermal conductivity of water based silver nanofluids”, International Journal of Thermal Sciences, 1-9.

[13] Jang S.P. and Stephen U. S. Choi, (2004), "Role of Brownian motion in the enhanced thermal conductivity of nanofluids", Applied Physics Letter volume 84, 4316

[14] Sadik Kakac, Anchasa Pramuanjaroenkij, (2009) , "Review of convective heat transfer enhancement with nanofluids", International Journal of Heat and Mass Transfer v o l . 52, 3187-3196.

[15] Cheng L, (2009), "Nanofluid heat transfer technologies",Recent Patents on Engineering, Vol. 3, No.1 .

[16] Shah R.K., Sekulic Dusan P., (2010), “ Fundamental of heat exchanger Design”, John Wiley & Sons. Inc., Sixth edition

[17] Kuppan T., (2010), “ Heat exchanger design hand book” Marcel Dekker Inc.

CHAPTER-2

Literature Survey

Durgeshkumar Chavan et al. [1] Al_2O_3 was used to prepare nanofluid and used in automobile radiator to study the enhanced heat transfer performance of radiator over pure water. Flow rate was kept between 3L/min to 8L/min and come under turbulent region. Nanoparticles were used in four different concentrations between (0-1) vol percent. Results showed that as the flow rate was increased heat transfer performance was increased. At 1% vol concentration 40-45% enhancement was achieved in heat transfer performance over pure water. As the particle size was reduced Brownian motion become more evident and this random motion increased the heat transfer rate of fluid.

Vermahmoudi Y et al. [2] had done experiment under laminar condition with Fe_2O_3/water nanofluid having concentrations 0.15%, 0.40%, 0.65% by volume. Nanofluids flow rate was 0.2 to 0.5 m^3/ hr at 50°C, 60°C and 80°C. Results shows that the nanofluids Reynolds number varied from 200 to 1000 and as the Reynolds number increased overall heat transfer coefficient increased but at constant Reynolds number overall heat transfer coefficient increased as the nanoparticles concentration increased. Air side Reynolds number is varied from 500 to 700. As the bulk movement of air the overall heat transfer coefficient increased and more energy is transferred from nanofluid to air. As the temperature of nanofluid increased the overall heat transfer coefficient decreased because of large LMTD. Around 13% enhancement is achieved at 0.65% concentration of nanoparticles as compared with distilled water.

Adnan M. Hussein et al. [3] done work experimentally and numerically to find the effect on friction factor and heat transfer enhancement by using SiO_2 nanoparticle in water. Four different concentrations were used range from 1 to 2.5 vol% concentration in water. Flow rates were varied from 2 l/min to 8 l/min with Reynolds number value lied between 500-1750. As the flow rate increased the value of friction factor decreased on the other hand the value of Nusselt number increased. There was significant increase in heat transfer coefficient

and friction factor with particle concentration. There was 22% enhancement in friction factor at 2.5% vol concentration and 40% enhancement in Nusselt number.

Hwa-Ming Nieh et al. [4] Used Al_2O_3 and TiO_2 nanoparticles in air cooled radiator to enhance the performance. Viscosity, thermal conductivity and specific heat of nanocoolant was measured at different nanoparticle concentration and then pressure drop, heat dissipation capacity, pumping power was evaluated at different flow rates. Results showed the relationship between pumping power and heat dissipation capacity with the help of efficiency factor. Efficiency factor and heat dissipation is higher for nanocoolant than Ethylene glycol/water mixture. TiO_2 showed the grater enhancement than Al_2O_3. Maximum enhancement ratio was 25.6% for heat dissipation rate, 6.1% enhancement for pressure drop, 2.5% enhancement for pumping power and efficiency factor has 27.2% enhancement as compared to Ethylene glycol/water mixture.

Adnan M. Hussein et al. [5] used TiO_2 and SiO_2 nanoparticles in water to prepare nanofluid used in radiator to investigate the heat transfer enhancement and performance. Flow rate was maintained from 2-8 Liter per Minute (LPM). Inlet temperature was varied from 60°C to 80°C. Nanoparticle concentration was 1% to 2% by volume. Results showed that as the Reynolds number increased the Nusselt number was increased. As the particle volume concentration was increased the value of Nusselt number was also increased. Results showed that SiO_2 nanofluid was better than TiO_2 nanofluid. Maximum value of Nusselt enhancement was 22.5% for SiO_2 nanofluid and 11% for TiO_2 nanofluid. Therefore SiO_2 nanofluid had better enhancement than TiO_2 nanofluid and TiO_2 nanofluid was better than water. Behavior of Nusselt number is depend upon the volume flow rate, inlet temperature and nanoparticle concentration in fluid.

Sandesh S. Chougle et al. [6] done experiment on car radiator by using carbon nanotubes (CNT) and Al_2O_3 nanoparticles in water with four different concentration range from (0.15 to 1 vol.%). Flow rate was varied between 2l/min to 5 l/min. Forced convective heat transfer performance was studied and results showed that at 1% vol. nanoparticle maximum heat transfer enhancement was 90.76% and 52.03% for CNT and Al_2O_3 nanofluid respectively was achieved. As the coolant mass flow rate increased heat transfer performance was increased for both the nanocoolant. CNT nanofluid showed massive enhancement as

compared Al_2O_3 nanofluid because CNT had high aspect ratio, high thermal conductivity, and low thermal resistance. As the concentration of nanoparticle was increased thermal conductivity was also increased hence cooling performance was also increased.

Naraki M et al. [7] took CuO/water nanofluids in car radiator under laminar condition ($100 \leq Re \leq 1000$) at 0.4 % concentration by volume and about 8% enhancement is achieved over distilled water. Due to increase in thermal conductivity and Brownian motion of nanoparticles enhancement was increased. Flow rate increment in nanofluids lead to increase in overall heat transfer coefficient but as inlet temperature of nanofluid increased from 50°C to 80°C overall heat transfer coefficient decreased. There were three factors for that decrement a) as the temperature increased viscosity of nanofluid decreased much greater than density which leads to higher Reynolds number. b) At low viscosity of nanofluids the particles alignment was very rapid leading to less contact between nanoparticles. c) Thermal conductivity become lower as the particles depleted near the wall surface. For air side Reynolds number as it increased the overall heat transfer coefficient increased.

Adnan M. Hussein et al. [8] done experiment and study the effect of tube cross sectional on heat transfer of car radiator to improve the radiator's cooling performance. With the help of fluent software CFD model was prepared based on finite volume technique. Three different types of shapes were considered and TiO_2 nanofluid was used at 1%, 1.5%, 2%, 2.5% concentration of nanoparticle. Circular elliptical and flat type tube cross section was considered with hydraulic diameter of 3mm and length 500mm. results showed that for circular cross section tube had higher friction factor than elliptical than flat tube. Friction factor decreased as the value of Reynolds number increased. Therefore heat transfer coefficient is higher for flat tube followed by elliptical tube followed by circular cross section of tube because for flat tube cross sectional area was more.

Madhursee kole et al. [9] used Al_2O_3 nanoparticle size < 50nm with oleic acid as surfactant. Nanofluid was stabled for 80 days and viscosity was found as the function of alumina concentration in base fluid. Temperature of nanofluid was kept between 10°C to 50°C. Results showed that viscosity of nanofluid increased as the concentration of nanoparticle was increased and decreased with increase in temperature. At small nanoparticle concentration

alumina showed Non-Newtonian behavior (Newtonian for pure engine coolant). Viscosity of nanofluid is given by expression:

$$\log(\mu_{nf}) = A\exp(BT). \quad (2.1)$$

A Vaisi et al. [10] studied the pressure drop and heat transfer in louvered fin compact heat exchanger. Geometrical parameters of louver fin, louvered pitch, and louvered arrangement were examined. Performance of compact heat exchanger was depended up on the geometric parameter. Results showed that there were decreased in pressure drop around 18% and enhancement in heat transfer was 9.3% when symmetrical arrangement was provided. Fin weight was reduced to17.6% because louvers were presented more in number per row for symmetrical pattern. Pressure drop was increased as the air velocity was increased for symmetrical pattern but for same velocity symmetrical louvered had less pressure drop. As number of fin decreased heat transfer area was decreased therefore cooling rate of fluid is more in symmetrical case.

Jahar sarkar et al. [11] used 20% ethylene glycol and 80% water to form ethylene glycol/water mixture (EG/water). Four type of nanoparticles are used Cu, SiC, Al_2O_3, and TiO_2 to see the effect of these particle in coolant for improvement in cooling capacity, effectiveness and reduction in pumping power. Results showed that SiC yield best result in performance in radiator followed by Al_2O_3, TiO_2 and Cu respectively. Maximum 15.34% enhancement in cooling capacity for SiC, 14.33% for Al_2O_3, 14.03% for TiO_2, 10.20% for Cu. Cooling capacity was increased as the mass flow rate of air was increased. This was happened because heat transfer coefficient increased and effectiveness was decreased. Results showed that Cu based nanofluid had least cooling capacity and effectiveness when compare to other. As mass flow rate of coolant increased cooling capacity and effectiveness was increased. Cu required less power for pump as compared to other when inlet temperature of nanofluid was increased. Heat transfer rate was increased but there was very small increment in effectiveness. For each nanofluid second law efficiency and effectiveness was improved.

Tun-ping teng et al. [12] done experiment on motorcycle radiator to investigate the performance of radiator by using multi-walled carbon Nanotube at different concentration

(0.1, 0.2 and 0.4 wt %) and cationic chitosan dispersant in ethylene glycol in 1:1ratio. Different temperature (80°C, 85°C, 90°C and 95°C) to study thermo physical properties of nanofluid at different flow rates (4.5, 6.5, and 8.5 L/min). Also calculate the overall efficiency with the help of efficiency factor and evaluate the relation between pumping power, heat exchanger capacity by using efficiency factor.12.8%, 4.9%, and 14.1% enhancement was achieved for heat transfer, pumping power, and efficiency factor respectively for all experiment.

Peyghambarzadeh et al. [13] used Al_2O_3 nanoparticles (average mean size 20 nm) in water and ethylene glycol and water-ethylene glycol in aluminum flat tube louver fin radiator. Heat transfer enhancement for pure ethylene glycol and pure water and water-ethylene glycol was compared at Different concentrations (0.1, 0.3, 0.5, 0.7, 1 % vol). Different temperature range was used (350C-500C) for water and (350C-600C) for ethylene glycol at different flow rate was varied from 2-6 L per min. Results showed that there was 40 % increase in heat transfer coefficient for both nanofluids. Nanofluids heat transfer behavior highly depended on different concentrations and different flow rates and slightly depended on temperature.

Peyghambarzadeh et al. [14] did experiment to study the heat transfer coefficient enhancement on car radiator with CuO and Fe_2O_3 at different concentrations with constant flow rate 10 L/min. De-ionized water is used and obtained data was compared with nanofluid's calculations and theoretical relations of heat transfer. Results showed that as the Reynolds number of air increased at constant temperature the overall heat transfer coefficient increased. But at same concentration and Reynolds number as the temperature increased the overall heat transfer coefficient decreased.

Navid Bozorgan et al. [15] γ-Al_2O_3 with 20 nm mean sized nanoparticles were used in water as coolant in automotive diesel engine radiator. Turbulent conditions were taken for overall heat transfer enhancement at different volume fractions. Results showed that at same concentration the pumping power decreased as the speed of vehicle increased, and at different concentrations the power increased as the concentration increased at same speed. Concentration increased the viscosity and density of nanofluid increased as a result pressure drop increased which lead to increment in friction factor.

Peyghambarzadeh et al. [16] investigated the heat transfer coefficient for automobile radiator with Al_2O_3-water nanofluid 20 nm mean sized particles and with pure water. Flow rate was kept constant 2-5 L/min. Temperature range was 37^0C - 49^0C at different concentrations (0.1, 0.3, 0.5, 0.7, 1.0 % vol). Results showed that as the concentration of nanoparticle increased outlet temperature of coolant decreased. As flow rate of coolant increased outlet temperature of coolant increased at same concentration. At 1% vol concentration enhancement become 45% because Nussle number increased as the Reynolds number increased.

Leong et al. [17] investigated the performance of heat transfer coefficient of car radiator with water and ethylene glycol as coolant. There was 3.8% enhancement in heat transfer coefficient with 2% concentration of copper nanoparticle in water when air Reynolds number is 6000 and for coolant it was 5000. When ethylene glycol was used as coolant with 2% concentration of copper nanoparticles only 0.9% enhancement was occurred at 4000 and 6000 Reynolds number for ethylene glycol and air respectively. 0.4% of enhancement was achieved when only ethylene glycol used as coolant. Power was increased by 12.13 % and reduction in frontal area was 18.7%.

Tk Dey et al. [18] did experiment on car engine coolant containing Al_2O_3 nanoparticle (< 50 nm nominal diameter). Surfactant oleic acid was used for suspension of nanoparticles more than 80 days at different temperature range (10^0C-80^0C). He investigated that viscosity and thermal conductivity both was function of particle concentration in nanofluid. Around 10.41% of enhancement was occurred at room temperature. Viscosity increased with increase in concentration of nanoparticle. An empirical correlation was given › $Log(\mu_{nf}) = Ae^{-BT}$ that tells about the dependence of viscosity on temperature. As concentration increased the thermal conductivity of nanoparticle was increased with increased in temperature. Maximum enhancement is around 11.25% at 80^0C at 0.035 concentration of Al_2O_3.

Pramod et al. [19] took six nanofluids for their experiment of different size and different volume fractions. As the size of nanoparticle decreased the thermal conductivity of nanofluid decreased. A correlation model of thermal conductivity with particle size was give through which they compared their experimental data.

$K_{eff}(L,T,\phi) / K_1(T) = [K_p(L,T) / K_1(T)]^{\phi}$

$K_{eff}(L,T,\phi)$ was the effective thermal conductivity of nanofluid as fuction of particle size, temperature, and concentration (L,T,ϕ) respectively. $K_1(T)$ was thermal conductivity of base fluid as a function of temperature. $K_p(L,T)$ was thermal conductivity of particle as a function of particle size and temperature.

Reza Azizian et al. [20] did experiment to investigate the mechanisms behind the enhancement in thermal conductivity of nanofluids. They take 70nm Al_2O_3 in water up to 13% concentration by volume and Tio_2 up to 5% concentration by volume. The heat transport mechanism inside the small size nanoparticle was ballistic heat transport and it occurred when temperature gradient becomes larger or when mean free path is larger than the sample size or nanoparticle size. Mean free path according to Debye theory is given by equation

$l=\frac{10aT_m}{\gamma T}$, Where 'l' is mean free path, 'a' is lattice constant, 'T_m' is melting temperature, 'γ' is gruneisen parameter, 'T' is temperature.

LotfizadehDehkordi et al. [21] done experiment by taking 60:40 mass ratio of ethylene glycol-water. SDBS was used as surfactant and its concentration effect on thermal conductivity and viscosity of Al_2O_3 nanofluid. Low concentration of SBDS (<1 wt %) is good for dispersion and enhanced the thermal conductivity of nanofluid. Higher concentration of SDBS (>1 wt %) lead to reduction in thermal conductivity of nanofluid and accelerate the viscosity augmentation of nanofluid. High concentration of SDBS influence the inter particle force in nanosuspension and produce foam in nanofluid which retard the thermal conductivity of nanofluid. Results also showed that the viscosity of nanofluid was temperature depended. As the volume concentration of nanofluid increased thermal conductivity increased with increase in temperature.

Das et al. [22] investigated the thermal conductivity enhancement with temperature of Al_20_3 CuO water-based nanofluids. Temperature Oscillation technique was used to measure the thermal conductivity. Average diameter of alumina particles was 38.4 nm and for CuO was 28.6 nm the experimental results showed that with increased in temperature thermal conductivity increased. Nanofluid containing smaller particles (CuO) showed

greater enhancement in thermal conductivity with temperature. Enhancement in conductivity also depended on particle concentration, as concentration increased thermal conductivity increased.

Murshed et al. [23] took two different shaped nanoparticles, one is cylindrical (φ10nm x 40nm) diameter by length and other one is spherical (φ 15 nm) in water (base fluid).experimental results showed that there is 30% to 33% enhancement in thermal conductivity at 5% volume fraction. The thermal conductivity was determined by transient hot wire method. To obtain better stability of nanoparticles, surfactant CTAB (Cetyl Trimethyl ammonium bromide) was used with concentration (0.01%-0.02%) without affecting the thermo physical properties of nanofluid. **It** kept nanoparticles dispersed by strong electrostatic repulsive force and hydrophobic surface force between particles due to physical adsorption of surfactant in solution. Results showed that small nanoparticle concentration in basefluid increased the enhancement in thermal conductivity. As the concentration increased thermal conductivity increased. Particle size also affects the conductivity. Cylindrical shaped particles have more thermal conductivity than spherical shape particles.

Arani et al. [24] investigated that the convective heat transfer coefficient and pressure drop was affected by particle concentration. Ti02 (30 nm) nanoparticle in deionised water is used, Reynolds number was between 8,000-51,000. As the Reynolds number was increased the Nusselt number also increased, but higher value of Reynolds number leads to high power consumption to compensate the pressure drop. Based on his experimental results they consumption to compensate the pressure drop. Based on his experimental results they concluded that, for a given Reynolds number Nusselt number increased as the concentration of nanofluid increased. Thermal performance of all Reynolds number is examined by using high concentration of nanofluid having high Nusselt number.

Xuan et al. [25] studied the effect of Cu nanoparticles concentration (with different volume fraction) on heat transfer enhancement. Coefficient of convective heat transfer increased with increased in flow velocity and volume fraction of nanoparticle for Reynolds

number between 10,000-25,000. **It** may be noted that the heat transfer coefficient was larger than that of base fluid alone at same flow velocity. At high concentration viscosity of nanofluid increased and holds back the heat transfer enhancement because as viscosity was increased turbulence in flow decreased. Energy transfer rate increased by random motion between the particles in suspension.

Abdulhassn et al. [26] measured pressure drop and convective heat transfer coefficient of water based Al (25 nm), Ab03 (30 nm) and CuO (50nm). They took one metallic nanoparticle and two metal oxide nanoparticles and compared to find which one was best in heat transfer. A circular tube in which nanofluid flows has fully developed laminar flow. Two cases were reported by their experimental study.

a) Test section without insulation.
b) Test section with insulation.

Result showed that the test section with insulation containing AI, Ab03, CuO nanoparticles with water has increase in Nusselt number (45%, 32%, and 25%) and for without insulation test section it is (36%, 23% and 19%) respectively. Metal nanoparticles Al showed more enhancement than oxide nanopartic1es Ah03 and CuO and CuO had least enhancement at same concentration. Enhancement in thermal conductivity depends on size, shape, concentration, fluid viscosity. As concentration increased thermal conductivity enhancement increased. When the particle size was decreased the random motion was larger and the convection like effect become dominant and thermal conductivity enhancement occur.

Jang et al. [27] observed that the Brownian motion played very important role in enhancement in thermal conductivity. Conductivity not only depend on temperature, concentration of particle' but also robustly depend on size of particles. Nanofluids have basically four modes of heat transfer (1) Base fluid molecules collision (conductivity of base fluid). (2) Thermal diffusion between nanoparticles. (3) Collision between nanoparticles due to Brownian motion. (4) Collision between nanoparticle and base fluid molecules. As the temperature increases base fluids viscosity decreases as a result the Brownian motion of nanoparticles increases and hence thermal conductivity increases.

When the particle size decreases, random motion between molecules is large and convection effect becomes dominant. Thermal conductivity increased as the volume fraction percentage increased.

W Evans et al. [28] said that the contribution of Brownian motion in enhancement of thermal conductivity is very small less than 1 %. For Brownian motion estimation they assumed that the velocity of particle is same as that of fluid and entire volume of fluid is diffused together with nanoparticles. Conductivity contribution by Brownian motion is given by,

$K_B = D_B C_P$, where K_B conductivity contribution by Brownian motion is, C_P is heat capacity per unit volume and D_B is thermal diffusivity of nanoparticles.

$K_F = D_F C_P$, similarly KF, D_F, Cp conductivity, diffusivity, heat capacity of fluid respectively.

KB/KF Ratio is very small (< 1 %) shows that the Brownian motion contribution is negligible at low concentration and not accountable for thermal transport.

Hong et al. [29] worked on Fe nanoparticle and observed the effect of clustering of nanoparticle. He observed that as the time of sonication increased thermal conductivity enhancement increases. Nanoparticles at high concentration easily agglomerate because distance is between the particles are reduced.

Murshed et al. [30] studied the thermal conductivity enhancement of Ti02 and Ah03 nanoparticles with water as base fluid affected by surfactant and nanoparticle cluster formation in base fluid. This happened commonly when two step process for preparation of nanofluid and these nanoparticle agglomerates settled down in container. Cluster formation is studied by using transmission electron microscope (TEM). He observed that as the concentration of nanoparticles is increased the agglomerate or cluster formation between nanoparticles is increased. This cluster formation reduced the thermal conductivity enhancement. Agglomerate formation depended on particle size, shape, concentration, viscosity of base fluid. Large size of cluster formation at high concentration leads to free region in base fluid and provide high thermal resistance which reduce the enhancement in

conductivity. Remedy for nanofluid clustering is sonication and surfactants. They break down the large agglomerate and offer stability in nanoparticles and enhance the thermal conductivity. Cetyl trimethyl ammonium bromide (CTAB) surfactant is used in small amount to make nanoparticles stabile and improve the dispersion behavior of nanoparticle, Adsorption of surfactant in fluid leads to electrostatic repulsive force and hydrophobic surface forces.

Michel P. Beck et al. [31] did the experiment on alumina nanoparticles in water and ethylene glycol base and found that if the particle size is below 50 nm the thermal conductivity enhancement decreases. This decrease in thermal conductivity enhancement is due to phonon scattering at solid-liquid interface. The correlation of thermal conductivity enhancement which depend on diameter of nanoparticle is given by

$$\epsilon = (k-k_1)/k_1 = \epsilon_{max} (1 - e^{-0.025d}) \quad (2.2)$$

$$\epsilon_{max} = 4.4134\ \varphi \quad (2.3)$$

$$\epsilon_{max} = 5.527\ \varphi \quad (2.4)$$

Where k is thermal conductivity of nanofluid, k_1 is thermal conductivity of base fluid, d is diameter of nanoparticle. φ is volume fraction. ϵ_{max} is limiting value of thermal conductivity at any volume fraction as particle size increases and equation (2.2) & (2.3) is for nanoparticles in water and ethylene glycol respectively.

V.Karthik et al. [32] suggested that the enhancement in thermal conductivity is contributed by phononic and electronic thermal transport was due to frequently collision between nanoparticles and heat source. The phononic transport was explained with the help of molecular dynamics (MD) approach when particle size is less than 15 nm and electronic transport is explained by meso-continuum model when particle size is greater than 15 nm. MD tells that the heat transfer by atom vibrations not by electronic movement and play dominant role in metallic heat transfer. Meso continuum tells the heat was gained when nanoparticles collide with heat source. Heat was exchanged between nanoparticle and base fluid continuously via convective heat transfer depending oil temp difference between moving particle and base fluid.

References

[1] Chavan Durgeshkumar, Pise Ashok T., (2014), "Performance Investigation of an Automotive Car Radiator Operated With Nanofluid as a Coolant", Journal of Thermal Science and Engineering Applications Vol. 6, 021010-1.

[2] Vermahmoudi Y, Peyghambarzadeh S.M, Hashemabadi S.H, Naraki M, (2014), "Experimental investigation on heat transfer performance Fe_2O_3/water nanofluid in an air-finned heat exchanger" , European Journal of Mechanics B/Fluids Vol. 44, 32–41.

[3] Hussein Adnan M., Bakar R.A., Kadirgama K., (2014), "Study of forced convection nanofluid heat transfer in the automotive cooling system", Case Studies in Thermal Engineering Vol. 2, 50–61.

[4] Nieh Hwa-Ming, Teng Tun-Ping, Yu Chao-Chieh, (2014) , "Enhanced heat dissipation of a radiator using oxide nano-coolant", International Journal of Thermal Sciences Vol. 77, 252-261.

[5] Hussein Adnan M., Bakar R.A., Kadirgama K., Sharma K.V., (2014), "Heat transfer enhancement using nanofluids in an automotive cooling system", International Communications in Heat and Mass Transfer Vol. 53, 195–202.

[6] Chougule Sandesh S., Sahu S. K., (2014), "Comparative Study of Cooling Performance of Automobile Radiator Using Al_2O_3-Water and Carbon Nanotube-Water Nanofluid", Journal of Nanotechnology in Engineering and Medicine Vol. 5, 011001-1.

[7] Naraki M, Peyghambarzadeh S.M, Hashemabadi S.H, Vermahmoudi Y, (2013), "Parametric study of overall heat transfer coefficient of CuO/water nanofluids in a car radiator" , International Journal of Thermal Sciences Vol. 66, 82-90.

[8] Hussein Adnan M., Sharma K.V., Bakar R.A., Kadirgama K., (2013) , "The effect of cross sectional area of tube on friction factor and heat transfer nanofluid turbulent flow", International Communications in Heat and Mass Transfer Vol. 47, 49–55.

[9] Kole Madhusree, Dey T.K., (2010), "Viscosity of alumina nanoparticles dispersed in car engine coolant", Experimental Thermal and Fluid Science Vol. 34, 677–683.

[10] Vaisi A., Esmaeilpour M., Taherian H., (2011), "Experimental investigation of geometry effects on the performance of a compact louvered heat exchanger", Applied Thermal Engineering Vol. 31, 3337-3346.

[11] Sarkar Jahar, Tarodiya Rahul , (2013), "Performance analysis of louvered fin tube automotive radiator using nanofluids as coolants", Int. J. Nanomanufacturing, Vol. 9, No. 1.

[12] Teng Tun-Ping , Yu Chao-Chieh, (2013), " Heat dissipation performance of MWCNTs nano-coolant for vehicle", Experimental Thermal and Fluid Science Vol. 49, 22–30.

[13] Peyghambarzadeh S.M., Hashemabadi S.H., Hoseini S.M., Seifi Jamnani M., (2011), "Experimental study of heat transfer enhancement using water/ethylene glycol based nanofluids as a new coolant for car radiators", International Communications in Heat and Mass Transfer Vol. 38, 1283–1290.

[14] Peyghambarzadeh S.M., Hoseini S.M., Naraki M., Vermahmoudi Y., (2013), "Experimental study of overall heat transfer coefficient in the application of dilute nanofluids in the car radiator" , Applied Thermal Engineering Vol. 52, 8-16.

[15] Bozorgan Navid, Krishnakumar Komalangan, Bozorgan Nariman, (2013), "The Performance Evaluation of Overall Heat Transfer and Pumping Power of γ-Al_2O_3/water Nanofluid as Coolant in Automotive Diesel Engine Radiator", ANUL XX, NR. 1, ISSN 1453 – 7397.

[16] Peyghambarzadeh S.M., Hashemabadi S.H., Hoseini S.M., Seifi Jamnani M., (2011), "Improving the cooling performance of automobile radiator with Al_2O_3/water nanofluid", Applied Thermal Engineering Vol. 31, 1833-1838.

[17] Leong K.Y., Saidur R., Kazi S.N., Mamun A.H., (2010), " Performance investigation of an automotive car radiator operated with nanofluid based coolants (nanofluid as a coolant in a radiator)", Applied Thermal Engineering Vol. 30, 2685-2692.

[18] Dey TK, Kole Madhusree, (2010), "Thermal conductivity and viscosity of Al2O3 nanofluid based on car engine coolant", J. Phys. D: Appl. Phys. Vol. 43, 315501 (10).

[19]Teja Amyn, Warrier Pramod, (2011), “Effect of particle size on the thermal conductivity of nanofluids containing metallic nanoparticles”, Nanoscale Research Letters, Vol. 6, 247.

[20] Azizian Reza, Doroodchi Elham, Moghtaderi Behdad, (2012), “Effect of Nanoconvection Caused by Brownian Motion on the Enhancement of Thermal Conductivity in Nanofluids”, Ind. Eng. Chem. Res., Vol. 51, 1782–1789.

[21] LotfizadehDehkordi B., Hamdi M., Ghadimi A., Metselaar H. S. C., Kazi S. N., Sadeghinezhad E., (2013), “Investigation of viscosity and thermal conductivity of alumina nanofluids with addition of SDBS”, Heat Mass Transfer Vol. 49, 1109–1115.

[22] S.K.Das, N. Putra, P. Thiesen and W. Roetzel., "Temperature dependence of thermal conductivity enhancement for nanofluids", -transactions of ASME. Journal of Heat Transfer Vol 125, 567-574.

[23] Murshed S.M.S, Leong K.C, Yang C., (2005), "Enhanced thermal conductivity of Ti02 water based nanofiuids", International Journal of Thermal Sciences Vol. 44, 367-373.

[24] Arani Abbasian A.A, Amani J, (2012), "Experimental study on the effect of Ti02-water nanofiuid on heat transfer and pressure drop" , Experimental Thermal and Fluid Science Vol. 42, 107-115.

[25] Xuan Yimin, Li Qiang, (2003), "Investigation on Convective Heat Transfer and Flow Features of Nanofluids", Journal of Heat Transfer, Vol. 125, 151-155.

[26] K. Abd. Abdulhassan, A1-Jabair Sattar, Sultan Khalid, (2012), "Experimental Investigation of Heat Transfer and Flow of Nano Fluids in Horizontal Circular Tube", World Academy of Science, Engineering and Technology Vol. 61.

[27] Seok Pil Jang and Stephen U. S. Choi, (2004), "Role of Brownian motion in the enhanced thermal conductivity of nanofluids" Appl. Phys. Lett., Vol. 84, 21.

[28] William Evans, Jacob Fish, Pawel Keblinski, (2006), "Role of Brownian motion hydrodynamics on nanofiuid thermal conductivity", Appl. Phys. Letters Vol. 88**,** 093116.

[29] K. S. Hong, Tae-Keun Hong, and Ho-Soon Yang, (2006), "Thermal conductivity of Fe nanofluids depending on the cluster size of nanoparticles", Appl. Phys. Lett. 88, 031901.

[30] S. M. Sohel Murshed, C. A. Nieto de Castro, and M. 1. V. Lourenco, (2012), "Effect of Surfactant and Nanoparticle Clustering on Thermal Conductivity of Aqueous Nanofiuids" Journal of Nanofiuids Vol. 1, 175-179.

[31] Michael P. Beck, Yanhui Yuan, Pramod Warrier, Amyn S. Teja, (2009), "The effect of particle size on the thermal conductivity of alumina nanofiuids" Journal of Nanoparticle Res Vol. 11,1129-1136.

[32] V. Karthik, S. Sahoo, S.K. Pabi, S. Ghosh, (2012), "On the phononic and electronic contribution to the enhanced thermal conductivity of water-based silver nanofiuids", International Journal of Thermal Sciences xxx, 1-9.

Chapter 3

Experimental setup and calibration

3.1 Introduction

Objective of the experiment was to study the **"Effect of Al_2O_3 / water nanofluid concentration on heat transfer and fluid flow characteristics in U-type flow cross flow compact heat exchanger".** Experimental set up was fabricated in Thapar University and experiments were done in Heat transfer lab. Experimental setup consist of cross flow heat exchanger, duct, fan, pump, storage tank, heating element, thermocouples, U-tube manometer, display unit , rotameter, bypass valve, PID controller as shown in Fig. 3.1 below

Fig. 3.1: Photograph of Experimental setup.

3.2 Layout of experimental setup

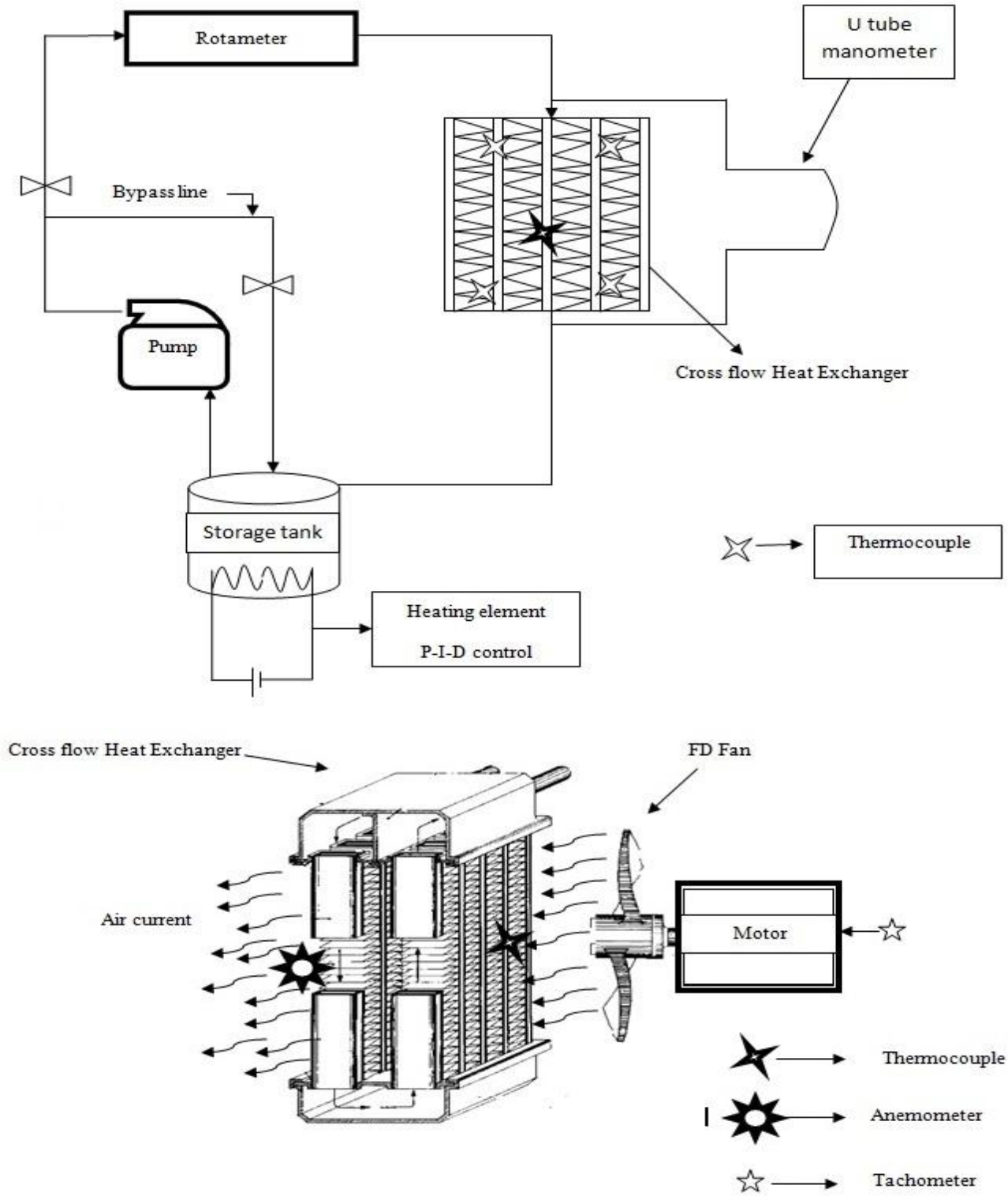

Fig. 3.2: Layout of experimental setup.

3.3 Requirements to run experimental setup

- Electricity, 220V, 50 Hz, 3 phase supply with voltage stabilizer.
- PID controller to regulate the current from heating element to maintained the temperature.
- Two pumps in water storage tank.

Table 3.1: Technical Data.

S.No.	Product	Specification
1	Cross flow heat exchanger	Copper fins multi louvered type and Brass tube. 2 rows each contain 14 tubes.
2	Duct	Made of GI sheet 18 gauge.
3	U-tube manometer	Pressure drop across radiator.
4	Rotameter	Capacity 0-60 LPH.
5	Temperature sensor	RTD PT-100 type.
6	Water tank	Stainless steel
7	Heating element	3000W power.
8	PID controller	SSR 25 LA, Fotek.
9	Anemometer	LT lutron AM- 4201 Anemometer

3.4 Test section

Test section contains U type flow compact cross flow heat exchanger which was made of copper fins and brass tubes as shown in Fig. 3.3. Heat exchanger was attached with a duct at one end and other end there was attached with a force draft fan, whose speed was changed with a changer. There were 14 tubes in one row and there are 2 rows presented in cross flow heat exchanger. Hot fluid was entered from upper pipe as shown in Fig. 3.3 in 14 tubes (first seven tubes (No. 1-7) in each row) from the left side, and flows in downward direction and collected in base of exchanger. After getting cool to certain temperature hot fluid flows in upward direction in next 14 tubes (No.8-14 in each row) leave the heat exchanger from right side. Specification of heat exchanger is given below in table 3.2.

Fig 3.3: Cross flow Heat exchanger

Table 3.2: Specification of cross flow heat exchanger.

Cross flow core dimensions	Height	240 mm
	Width	140.5 mm
	Thickness	30mm
Fin per inches	FPI	24

Radiation Areas	Tube	0.207 m^2
	Airways	1.683 m^2
	Total	1.890 m^2
Front Face Area	Total	0.033 m^2

Fin Length	1741 mm
Fin Width	30 mm
Fin Thickness	0.05 mm
Fin Type	Multi Louver

Tubes Rows	No.	2
Tubes	Total	28
Tube Thickness		0.14 mm
Tube Space		7.30 mm

3.5 Duct

Duct was made from GI sheet of 18 gauges as shown in Fig.3.4. Cross section of duct was 0.240×0.1409 m^2 and having uniform cross section length of 1.25 m for uniform flow of air, and 0.25m length is converging part. Duct was sealed with White stiff shuch that there was no air leakage occur from any joint made in duct. There was a honey combed structure placed to achive uniform flow inside the duct. Structure was placed where the converging part endes.

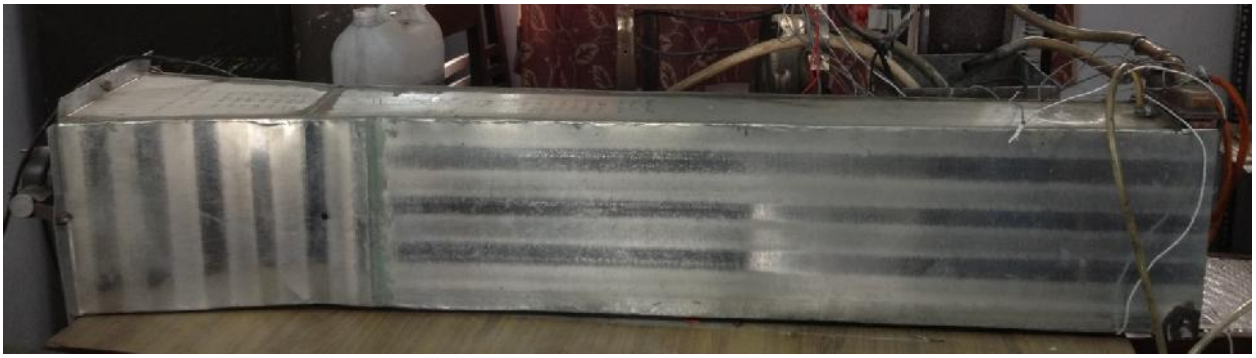

Fig. 3.4: Duct made of GI sheet.

3.6 Diffrential U tube manometer

Diffrential U tube manometer was used in setup to measure the pressure drop between inlet and outlet for hot fluid medium (Water and nanofluid), and for cold fluid medium (Air) in cross flow heat exchanger. Distilled water was used in limbs of U tube manometer, because its senstivity was high to measure the small pressure drop, measured by the difference between the heights of liquid in both limbs. The differential U-tube manometer is shown in Fig. 3.5

Fig. 3.5: U-tube manometer.

3.7 Collecting tank and Heating element

Collecting tank was made of stainless steel in which a heating element was placed to heat the working fluid. Collecting tank or storage tank has a capacity of 5.5 liters. Pump was placed in collecting tank to circulate the hot fluid whose temperature was sensed by thermocouple. Heating element of 3000W was used to heat the working fluid. It was small and in spiral shape fitted in storage tank. Heating element current was regulated by a PID controller. Fig. 3.6 shows both collecting tank and heating element.

Fig. 3.6: Collecting tank and Heating element

3.8 PID controller [1]

"Proportional-Integral-Derivative (PID) control is the most common control algorithm used in industry and has been universally accepted in industrial control. As the name suggests, PID algorithm consists of three basic coefficients; proportional, integral and derivative which are varied to get optimal response. The proportional component depends only on the difference between the set point and the process variable. This difference is referred to as the Error term. The proportional gain (K_C) determines the ratio of output response to the error signal. The integral component sums the error term over time. The result is that even a small error term will cause the integral component to increase slowly. The integral response will continually increase over time unless the error is zero, so the effect is to drive the Steady-State error to zero. The derivative component causes the output to decrease if the process variable is increasing rapidly. The derivative response is proportional to the rate of change of the process variable. Increasing the derivative time (T_d) parameter will cause the control system to react more strongly to changes in the error term and will increase the speed of the overall control system response". PID controller was shown in Fig. 3.7.

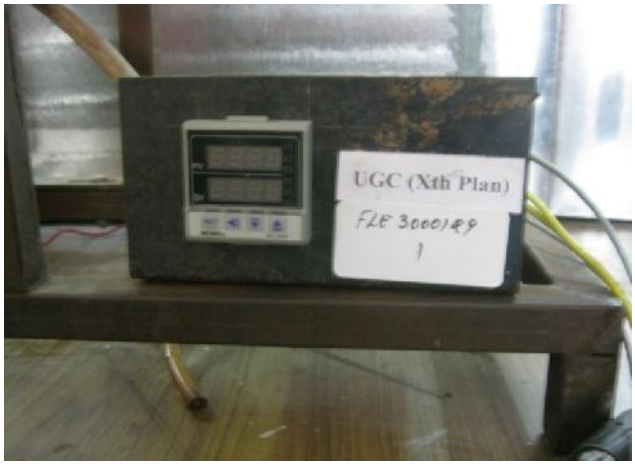

Fig. 3.7: PID controller.

3.9 Pump

A pump was used as shown in Fig.3.8 in flow circuit to circulate the hot fluid medium. Another pump was fitted in storage tank to circulate the water in tank itself so that when nanofluid was used, it remains in suspension in base fluid. Second pump also act as agitator which avoid evaporation and local heating of fluid near the surface of heating element. Specification of pump is given below in table 3.3

Table 3.3: Specification of pump [2]

Power consumption”	18W
Voltage	AC 220V, 50Hz
Outlet nozzle size	½ inch or 12.72mm
Maximum head	1.55m or (5 Ft.)
Maximum flow	750 L/H
Maximum cooler Height	1.25m or (4 Ft.)

Fig. 3.8: Pump

3.10 Rotameter

Rotameter was used to measure and control the flow rate of working fluid. It based on the principle of variable area, consist of three parts i.e. uniformly tapered flow tube, measurement scale, and a float. “Float was lifted up when fluid is passed through it and flow was controlled by a control valve placed at bottom of rotameter or at entry to rotameter. Bottom side of rotameter have smallest diameter and it increased as the tube length increased. As float goes up more and more fluid was passed through it because of increased variable area. When float become stable (means its weight is balanced by fluid upward thrust), the position corresponds to a point on the tube’s measurement scale provides an indication of the fluid’s flow rate” as shown in Fig 3.9 below

Fig. 3.9: Rotameter.

Flow rate is calculated with the help of a stopwatch and a measuring beaker. First the flow rate is set in rotameter and then takes readings with stopwatch. 1LPH is equal to 16.667 ml/min. therefore all flow rates are converted in ml/min. 25 LPH is equal to 416 ml/min. Similarly 30 LPH, 35 LPH, and 40 LPH equals to 500ml/min, 584 ml/min, and 667 ml/min respectively.

Table 3.4: Flow rates readings for calibration of Rotameter.

Flow rate ml/min	TEST 1 ml/min	TEST 2 ml/min	TEST 3 ml/min	TEST 4 ml/min	TEST 5 ml/min	TEST 6 ml/min	TEST 7 ml/min	TEST 8 ml/min	TEST 9 ml/min
416	418	420	419	417	419	421	420	419	420
500	510	509	507	506	505	505	504	503	505
584	588	587	588	591	591	592	587	588	586
667	670	670	670	671	671	670	670	670	670

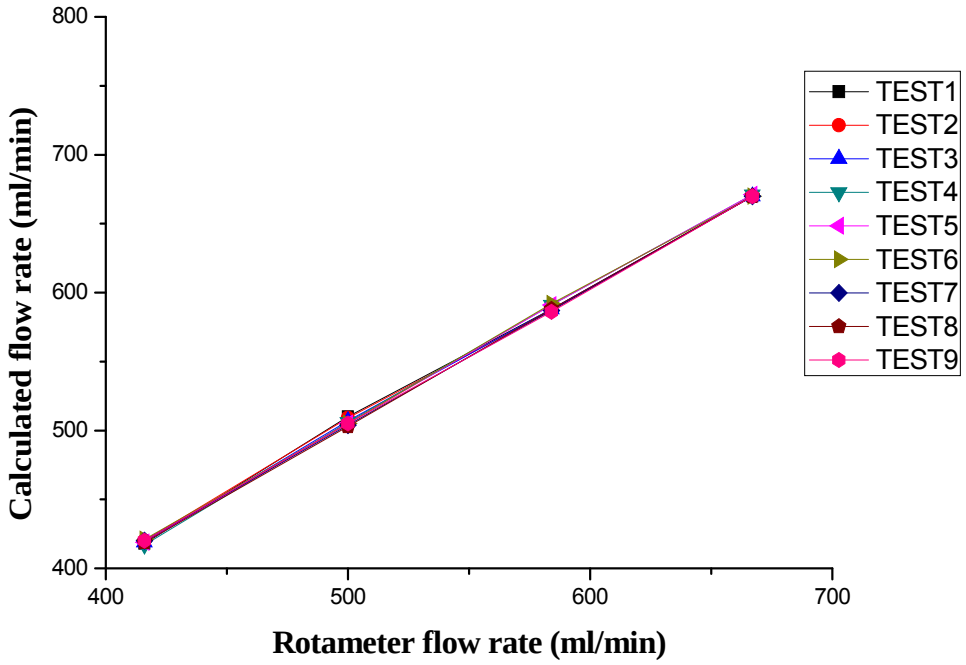

Fig. 3.10: Rotameter calibration graph.

3.11 RTD Pt 100 Thermocouple

RTD stands for resistance temperature detector as shown in Fig. 3.11. Resistance of conductor changes linearly with temperature as large as possible. Material of conductor has high resistivity so minimum value of material is used for RTD. Pt stands for platinum and 100 is platinum's resistance at 0°C temperature. Platinum is withstand with high temperature and is used most commonly due to purity, consistency/predictability, and high stability. It offers excellent accuracy over a wide temperature range (from-200 to +850 °C). There was ten thermocouple installed on cross flow heat exchanger to get the air side and water side temperature readings, four thermocouples are inserted in heat exchanger to measure the hot fluid temperature at inlet and outlet. Two thermocouples are inserted in header of heat exchanger at inlet and outlet and two are inserted in bottom collecting tank of exchanger. Six thermocouples were installed on surface of heat exchanger to get air side readings. Four in front side called air outlet and two on back side called inlet of heat exchanger respectively.

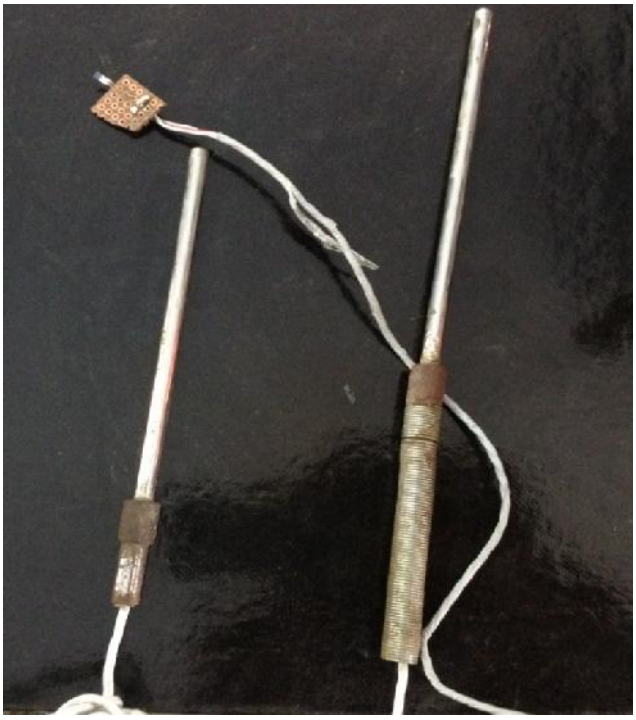

Fig. 3.11: RTD Pt 100 thermocouples.

Calibration on these ten thermocouples had been done and calibration chart and graph is given below in Fig 3.12 and table 3.5 respectively. Deviation is around $\pm$ 1°C to $\pm$ 1.5°C.

Table 3.5: Temperature readings of all thermocouple are for calibration.

Thermometer reading (°C)	RTD 1 (°C)	RTD2 (°C)	RTD3 (°C)	RTD4 (°C)	RTD5 (°C)	RTD6 (°C)	RTD7 (°C)	RTD 8(°C)	RTD 9(°C)	RTD1 0(°C)
18	18.7	18.3	18.9	18.2	18.6	18.8	18.5	17.3	17.9	19
18.5	19.2	18.9	19.1	18.7	19.4	19.3	19.1	17.9	18.3	19.4
19	19.6	19.3	19.6	19.4	19.6	19.9	19.6	18.4	18.7	19.8
19.5	20.1	19.9	20.1	19.8	20.2	20.3	20.1	18.8	19.1	20.4
20	20.8	20.4	20.7	20.5	20.8	20.8	20.7	19.4	19.6	20.8
40.5	41.2	40.8	41.4	41	41.1	41.2	41.3	39.7	40.2	41.3
43.5	44.1	43.9	44.3	43.8	44.4	44.1	44.1	42.8	43.1	44.4
45.5	45.9	45.8	46.2	45.7	46.2	46.3	46.2	44.9	45.3	46.2
55	55.8	55.5	55.9	55.3	55.8	55.9	55.6	54.4	54.7	55.9
55.5	56.3	56.1	56.4	55.9	56.2	56.4	56.1	54.7	55.2	56.2
66	66.7	66.4	66.9	66.4	66.8	66.7	66.6	65.3	65.7	66.8
66.5	67.2	66.9	67.5	66.8	67.1	67.2	67.2	65.9	66.4	67.3
70	70.7	70.4	70.9	70.2	71	70.6	70.6	69.4	69.8	70.7
89	89.7	89.6	89.9	89.3	89.8	89.7	89.7	88.3	88.7	89.6
90	90.8	90.2	91	90.6	90.9	90.7	90.6	89.2	89.7	90.8

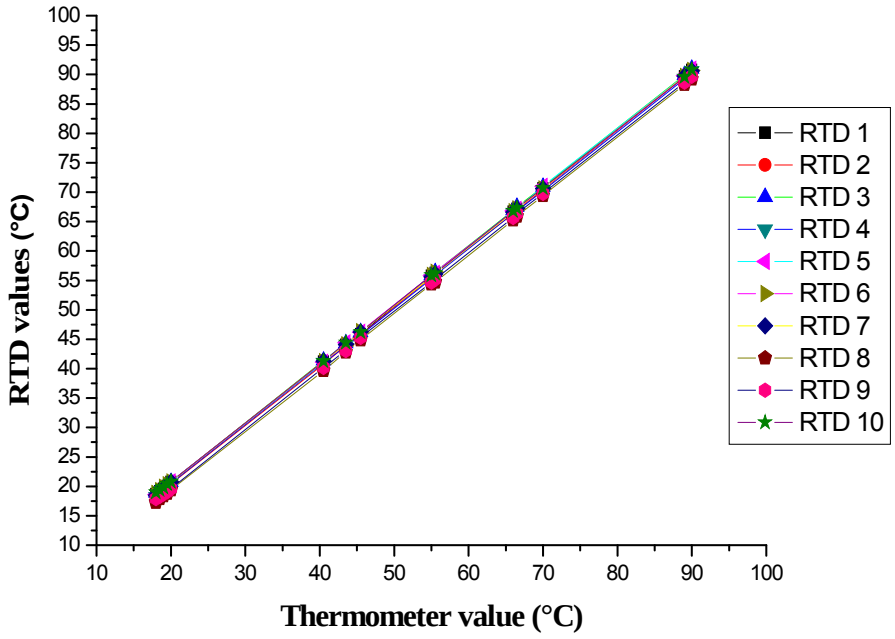

Fig. 3.12: RTD calibration graph.

3.12 Instruments used for nanofluid preparation and for calculation of thermo- physical properties.

3.12.1 Ultra sonicator water bath

Ultra sonicator (as shown in Fig. 3.13) which produced ultrasonic sound wave energy to agitate the nanoparticles in base fluid, and to make them in suspension for longer time period. Sonication can be used to speed dissolution, by breaking intermolecular interactions [2, 3].

Fig. 3.13: Ultra sonicator water bath.

3.12.2 Specific gravity bottle

Pycnometer or specific gravity bottle method was used to measure the specific density of nanofluid. Specific gravity is ratio of density of any fluid to density of distilled water at 4^{o}C temperature. Specific gravity bottle holds a specific volume at a particular temperature. There is a capillary hole in the close fitted ground glass stopper of specific gravity bottle as shown in Fig. 3.14 below. At a given temperature the extra liquid is released from the capillary for top filled bottle and remaining liquid's volume and weight was measured. Now weight of empty bottle is measured, the difference in weight is divided by the weight of distilled water of equal volume, which will give specific gravity of given liquid.

Fig. 3.14: Pycnometer.

3.12.3 Thermal properties analyzer KD2 PRO [2, 4]

Thermal conductivity of nanofluid is measured by KD2 PRO. It consists of panel which is hand handler type and a sensor which is inserted in medium, through which thermal conductivity is measured. There are two types of sensors single-needle and dual-needle. Single-needle sensor measures thermal conductivity and resistivity, while dual-needle sensor measures specific heat and diffusivity as shown in Fig. 3.15 below and specification of KD2 PRO are given below in table 3.6.

Fig. 3.15: KD2 PRO

Table 3.6: Specification for KD2 PRO.

Controller	-50 to +150 °C
Power	4 AA cells
Battery life	At least 500 readings in constant use or 3 years with no use (battery drain in sleep mode < 50 μA)
Case size	15.5 cm x 9.5 cm x 3.5 cm
Display	3 cm x 6 cm, 128 x 64 pixel graphics LCD
Keypad	6 key, sealed membranes
Data storage	4095 measurements in flash memory (both raw and processed data are stored for download)
Interface	9-pin serial
Read modes	Manual and Auto Read

Single-needle KS-1 60 mm small sensor as shown in Fig. 3.16 is used to measure the thermal conductivity and resistivity of fluid. The small size of the needle is designed primarily for liquid samples and insulating materials, which have short heating time. A very small amount of heat is applied to the needle which helps to prevent free convection in liquid samples. Specification of KS-1 sensor is given below in table. 3.7

Fig. 3.16: Single-needle sensor.

Table 3.7: Specification single-needle (KS-1)

Size	1.3 mm diameter x 60 mm long
Range	0.02 to 2.00 W/(m· K) (thermal conductivity) 50 to 5000 °C-cm/W (thermal resistivity)
Accuracy (Conductivity)	± 5% from 0.2 - 2 W/(m· K) ±0.01 W/(m· K) from 0.02 - 0.2 W/(m· K)
Cable length	0.8m

3.12.4 Brookfield DV-III Rheometer [2, 5]

Viscosity of nanofluid is measured from Brookfield DV-III Rheometer. Viscosity of fluid is measured of resistance occurs during flow. It gives fluid parameter like shear stress and viscosity at given shear rate. The principle of operation of the DV-III is such that the spindle is driven through a calibrated spring, which measures the viscous drag of the fluid against the spindle is by the spring deflection. A rotary transducer is used to measure the spring deflection. Rotational speed of the spindle measures the range of a DV-III in centipoises as shown in Fig. 3.17 and specification are given in table 3.8.

Fig. 3.17: Brookfield DV-III Rheometer.

Table 3.8: Specification Brookfield DV-III Programmable Rheometer.

Speed Range	0-250 RPM, 0.1 RPM increments
Viscosity Accuracy	±1.0% of full scale range for a specific spindle running at a Specific speed.
Temperature sensing range	- 100°C to 300°C (-148°F to 572°F)
Temperature accuracy	±1.0°C from -100°C to 150°C ±2.0°C from +150°C to 300°C
Analog torque output	0 - 1 Volt DC (0 - 100% torque)
Analog temperature output	0 - 4 Volts DC (10mv / °C)

References

[1] *PID controller* [online]. Available: http://www.ni.com/white-paper/3782/en/

[2] Gangacharyulu D., Sharma S., Kumar S., (2013), "Some studies of heat transfer and pressure drop characteristics of CuO-distilled water based nanofluid", M. Tech Dissertation, T.U., Patiala.

[3] Gangacharyulu D., Sharma S. Singh Kamaldeep, (2013), "Some studies of heat transfer and pressure drop characteristics of thermal energy storage system with Al_2O_3 nanofluid", M. Tech Dissertation, T.U., Patiala.

[4] KD2 Pro Thermal Properties Analyzer, Operator's Manual (Version 10), supplied by Decagon Devices, Inc., WA 99163 USA.

[5] Brookfield Digital Viscometer, Model DV-E, Operating Instructions, Manual No. M/98-350-g0307, Brookfield Engineering Laboratories, Inc., 11 Commerce Boulevard, Middleboro, MA 02346 USA

Chapter 4

Experimental work and calculation

4.1 Introduction

Cross flow heat exchanger are widely used in power sector, automotive industries, HVAC, etc. Performance of heat exchanger plays very important role. Heat transfer from hot medium to cold medium is always a challenging task. Main aim of this study is to enhance the heat transfer rate between hot fluid and cold fluid. Al_2O_3 nanoparticles were used at different concentration for this purpose to enhance the thermo physical properties of hot fluid; as a result heat transfer enhancement is achieved.

4.2 Preparation of nanofluids

The α-Al_2O_3 nanoparticles of average size 20nm were purchased from Intelligent Materials Pvt. Ltd, Panchkula. The properties of Al_2O_3 nanoparticles are given in table 4.1. XRD and TEM images are given in Annexure.

Table 4.1: Properties of the Al_2O_3 nanoparticles [1]

Chemical Name	α-Al_2O_3 nanopowder
Appearance	White powder
Purity	>99%
Average particle size	40nm
P^H	6.6
Density (Kg/m^3)	3970

Nanofluids are prepared by two step process. The nanoparticles are dispersed into the base fluid i.e. water. Make the volume concentration of 0.1%, and 0.2% by mixing 0.1945 gm, and 0.389 gm of nanoparticles in 50 ml of water respectively. To make the nanoparticles more stable and remain more dispersed in water ultra sonicator is used. Sonication had done for 3 hours before testing thermal conductivity& viscosity of the nanofluids. By this nanoparticles become more evenly dispersed in water. The Al2O3 samples prepared are as shown in Fig. 4.1 is as show below

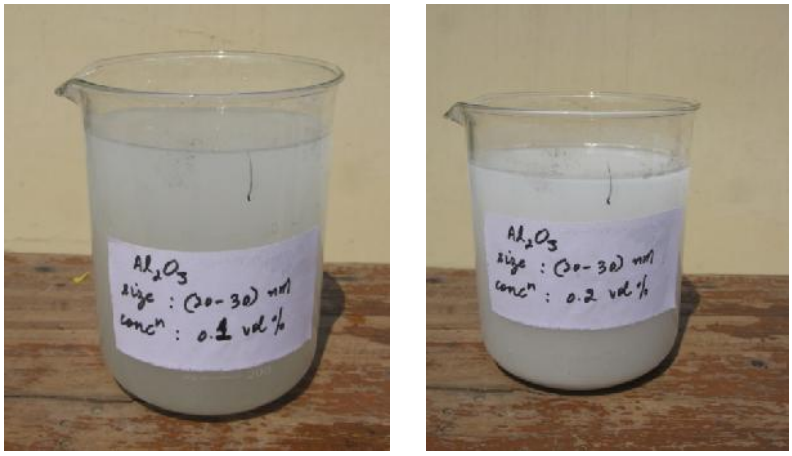

(a) (b)

Fig.4.1: (a) 0.1% concentration of nanofluid, (b) 0.2% concentration of nanofluid.

4.3 Experimental procedure

Experimental setup consist of a cross flow heat exchanger placed at one end of duct whose other end consist of force draft fan, having different rpm to change the velocity of air. Duct is 1.25 m long to produce the uniform flow of air through cross flow heat exchanger. Water tank consist of heater of 3000W who's current and voltage is regulated by PID controller. Heater heats the fluid flowing to heat exchanger through a pump. Thermocouples are mounted on heat exchanger to get the air side temperature readings, and four thermocouples are inserted in heat exchanger to measure the hot fluid temperature at inlet and outlet. Two thermocouples are inserted in header of heat exchanger at inlet and outlet and two are

inserted in bottom collecting tank of exchanger. A U-tube manometer is used to calculate the water side pressure drop.

Above mentioned experimental setup is used for heat transfer rate calculations and pressure drop calculations which are described as follows.

1. Electrical heater is switched on which is connected with PID controller to maintain the target inlet temperature. Three temperatures are taken 45°C, 50°C, and 55°C. First we take 45°C temperature for readings.
2. Pump is used to circulate the hot fluid in heat exchanger circuit as described in previous chapter.
3. Hot fluid consists of simple distilled water and nanofluid which contain Al_2O_3 nanoparticle at 0.1% conc. and 0.2% conc. in distilled water.
4. Another pump is used as agitator to regulate the suspension of nanoparticle in base fluid, and avoid the local heating phenomenon of fluid near the heater boundary to maintain the same temperature at every location in water tank.
5. First take distilled water as hot fluid for experimental procedure. Distilled water readings then compare with nanofluid readings to compare and see the enhancement in heat transfer rate.
6. Set the flow rate of hot fluid flowing in heat exchanger. Four different types of flow rates are taken i.e. 25, 30, 35, and 40 LPH respectively. Now set 25 LPH flow rate for readings.
7. Set the bypass line valve to get minimum flow rate through it such that maximum flow occurs through rotameter which is set at a particular flow rate.
8. Switched on the fan and set the velocity at which the readings will be taken. There are seven different velocities of fan i.e. 2.00 m/sec, 3.30 m/sec, 4.50 m/sec, 5.30 m/sec, 5.75 m/sec, 5.85 m/sec, 6.00 m/sec. For experimental readings set velocity at 2.00 m/sec.
9. Take reading after every 15 min of all the temperature sensors through a digital temperature indicator. Pressure drop readings are taken from U tube manometer for both hot fluid and cold fluid.
10. Repeat the process of readings till steady state is achieved.

11. Take two readings after steady state and note down all the values of temperature.
12. Change the flow rate of hot fluid 30, 35, and 40 LPH and repeat the same procedure at same speed.
13. Change the speed of fan to 3.30 m/sec after taking the values of temperature at all flow rate of hot fluid at steady state and repeat the procedure.
14. When all speeds are done then change the temperature to 50°C and repeat the same procedure for given temperature.
15. Repeat the same procedure for 55°C temperature and take the readings at steady state.
16. Take readings with nanofluid at 0.1% conc. for all flow rates, all speed, and all temperature.
17. Repeat the experiment with 0.2% concentration of nanofluid at all flow rates, all speed, and at all temperature.

4.4 Experimental calculations

Experimental calculations: calculations were done for both water side and air side at 45°C temperature of hot fluids. Air side thermo physical properties were taken at bulk mean temperature of air passing through heat exchanger when hot fluid is flowing inside it. Hot fluid's thermo physical properties were taken at bulk mean temperature. Consider a control volume as shown in Fig.4.2 to calculate the different types of area.

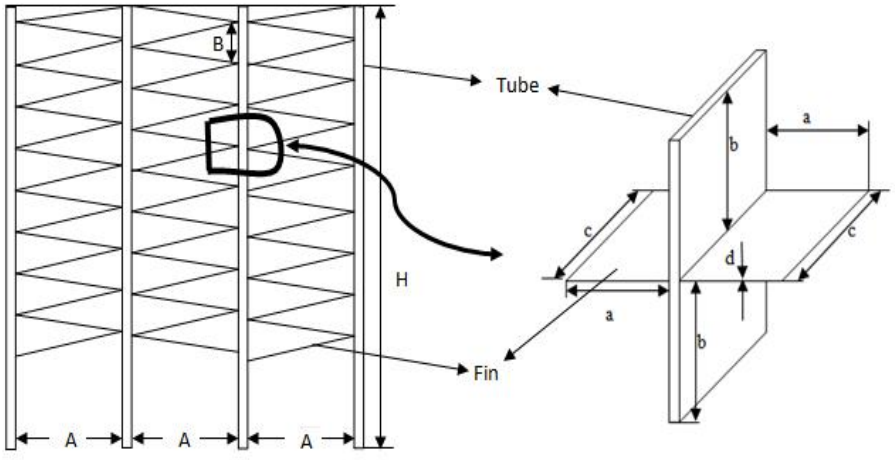

Fig. 4.2 Tube fin control volume.

4.4.1 Air side calculations

Air side calculation and its thermo physical properties are given below.

$D_{h,a}$ = 0.003854314 m μ_a = 18.8360 $\times 10^{-6}$ NS/m^2 ρ_a = 1.1154 Kg/m^3 P_r = 0.71

K_a = 0.0260 W/mK $C_{p,a}$ = 1013.35 J/Kg K Velocity of air = V_a = 2 m/sec

Mass flow rate of air = W_a Kg/sec

$$W_a = \rho_a \times A_c \times V_a \quad (4.1)$$

$$W_a = 1.1154 \times 0.011956 \times 2$$

$$W_a = 0.02667 \text{ Kg/sec}$$

Heat capacity rate = $W_a \times C_{p,a}$ (4.2)

$$W_a \times C_{p,a} = 27.028$$

Core mass velocity = G_a

$$G_a = W_a/A_c = 2.2305 \quad (4.3)$$

$$Re_a = G_a \times D_{h,a}/\mu_a \quad (4.4)$$

$$Re_a = \frac{2.2305 \times 0.003854314}{18.8360 \times 10^{-6}}$$

$$Re_a = 456.414$$

Reynolds number louvered side = Re_{lp}

$$Re_{lp} = \rho_a \times V_a \times l_p/\mu_a \quad (4.5)$$

$$Re_{lp} = 142.119$$

Colburn factor (J_a) is dimensionless representation of heat transfer coefficient [2]

$$J_a = 0.249 \times Re_{lp}^{-0.42} \times l_h^{0.333} \times H^{0.26} \times l_l^{1.1}/H_f^{1.1} \quad (4.6)$$

$$J_a = 0.249 \times 0.1247 \times 0.1473 \times 0.2336 \times 9.9218$$

$$J_a = 0.01060$$

$$h_a = J_a \times G_a \times C_{p,a}/Pr_a^{2/3} \quad (4.7)$$

$$h_a = 30.10733$$

$$m = \sqrt{2 \times h_a/K_a \times \delta} \quad (4.8)$$

$$m = \sqrt{60.21466/0.01995}$$

$$m = 54.93886$$

$$ml = 54.93886 \times 0.003725$$

$$ml = 0.204647$$

Fin efficiency η_f is given by equation (4.9)

$$\eta_f = \tanh ml/ml \quad (4.9)$$

$$\eta_f = 0.201837/0.204647$$

$$\eta_f = 0.9862$$

Overall efficiency η_0 is given by equation (4.10)

$$\eta_0 = 1.0 - (1.0 - \eta_f) \times {}^{A_f}/_{A} \quad (4.10)$$

$$\eta_0 = 1.0 - (1.0 - 0.9862) \times {}^{0.710283}/_{0.79113132}$$

$$\eta_0 = 0.9876$$

Overall heat transfer coefficient = U_a [2]

$$1/U_a = \frac{1}{\eta_0 \times h_a} + \frac{1}{(\alpha_w/\alpha_w) \times h_w} \quad (4.11)$$

$$1/U_a = \frac{1}{0.035300} = 28.32$$

Pressure drop of air side is given below [2]

$$\Delta P_a = P_i \times G_a^2/(2 \times P_i \times \rho_i) \times [(1 - \sigma_a^2) + 2 \times \{(\rho_i/\rho_o) - 1\} + \left(f \times E \times \frac{\rho_i}{r_h}\right) \times (1/\rho_m) - (1 - \sigma_a^2)(\rho_i - \rho_o)]$$

$\Delta P_a = 1.0665806$ pa.

$1/\rho_m = (1/\rho_i + 1/\rho_o)/2$ (4.12)

4.4.2 Hot fluid side

Hot fluid side calculation and thermo physical properties are given below

$D_{h,w}$ = 0.002795552 m μ_w = 719.8 $\times 10^{-6}$ NS/m^2 ρ_w = 994 Kg/m^3 $P_{r,w}$ = 4.81596

$K_w = 0.624$ W/mK $C_{p,w} = 4175$ J/Kg

Mass flow rate of water = W_w Kg/sec

$W_w = \rho_w \times V_f$ (4.13)

$W_w = 0.00690$ Kg/sec

Heat capacity rate = $W_w \times C_{p,w}$ (4.14)

$W_w \times C_{p,w} = 28.8075$

Core mass velocity = G_w

$G_w = W_w/n \times A_c = 24.450$ (4.15)

$Re_w = G_w \times D_{h,w}/\mu_w$ (4.16)

$$Re_a = \frac{24.450 \times 0.002795552}{719.8 \times 10^{-6}}$$

$Re_a = 94.954$

$h_w = K_w \times Nu_w/D_{h,w}$ (4.17)

$h_w = 1448.645$

$\Delta P_w = G_w^2 \times f_w \times H/2 \times \rho \times (D_{h,w}/4)$ (4.18)

$\Delta P_a = 22.41322$ pa

$\in = C_h \times (T_{h,i} - T_{h,o})/C_{min} \times (T_{h,i} - T_{c,i})$ (4.19)

$\in = 0.785289$

References

[1] Intelligent material Pvt. Ltd. www.nanoshel.com.

[2] Gangacharyulu D, Sharma J.K., Singh G, "Performance evaluation of after cooler in diesel engines- A case study" , IE(I) journal-MC, Vol 80, May 1999.

Chapter-5

Results and Discussions

5.1 Introduction

Experiments were conducted to measure the thermo physical properties of nanofluid, rate of heat transfer between hot fluid and cold fluid, and pressure drop across heat exchanger for both hot fluid and cold fluid. Thermo physical properties were measured by instruments like KD2 PRO, Brookfield DV-III, and pycnometer or specific density gravity bottle for thermal conductivity, viscosity, and density respectively. Temperature readings were taken to calculate the heat transfer rate for both hot fluid and cold fluid. Pressure drop was measured by using U-tube manometer. Heat exchanger has a U type flow through it, so it can be divided in two sections (a) hot section and (b) cold section. Hot section having downward flow from header inlet to base collecting tank of heat exchanger for hot fluid, and cold section have upward flow from base collecting tank to header outlet of heat exchanger as shown in Fig.5.1 below.

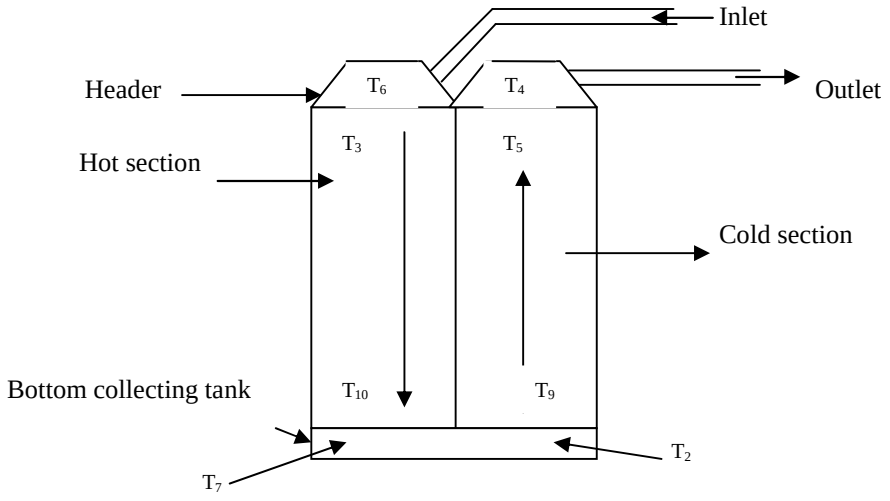

Fig. 5.1: Location of thermocouples on heat exchanger showing both hot and cold section respectively.

Inlet and outlet section are in the header section of heat exchanger. Fluid entered through inlet in header section at a given temperature T6 and flow was in downward direction through tubes, and gets cooled to T_7 when reached in bottom collecting tank. From bottom collecting tank fluid which is at temperature T_2 almost equal to T_7 start rising toward outlet. The heat exchanger is made of copper fins and brass tubes having high thermal conductivities, and also inlet and outlet in header section is made one continuous section separated by insulated material from inside. Due to this reason the temperature of fluid rises to T_4 from T_2 because heat is radially or transversely moved toward cold section through hot section. On the basis of above geometry followings are results discussed below.

5.2 Hot section heat transfer and fluid flow characteristics

5.2.1 Fin (Air) side Analysis

Fins of cross flow heat exchanger are multi louvered and made from copper material and tubes are made from brass. When air passes over the multi louvered fins it carries away the heat of hot fluid flowing inside the tubes. Thermal boundary plays a very important role in heat transfer rate. Flow is almost aligned over the multi louvered surface area and directed as the direction of louvered fin. The thermal fields in this region are quite uniform. Thinner the thermal boundary layer higher the heat transfer rate between the fins. Thinner boundary layer occurred at high velocity of air. Fin side heat transfer was studied by Colburn factor, which is dimensionless heat transfer coefficient and friction factor [3].

As the surface area for multi louvered fin is high, friction is quite significant between air and fin. Friction factor is high as most flow is louvered directed. It increased the heat transfer rate, as the cost of increased pressure drop. Multi louvered fins break the thermal boundary layer and increase the heat transfer rate. Heat transfer coefficient and friction factor both influence the thermal hydraulic performance.

Colburn factor is function of Stanton number and Prandtl number, and as shown in Fig. 5.2 Colburn factor of air decreases as Reynolds number increases of air for base fluid i.e. water. This happened because Stanton number which is a modified Nusselt number decreases as the Reynolds number increases. Whereas friction factor also decreases as the Reynolds number increases. As the surface area for multi louvered fin is high, friction becomes high. Friction factor is high as more flow is louvered directed.

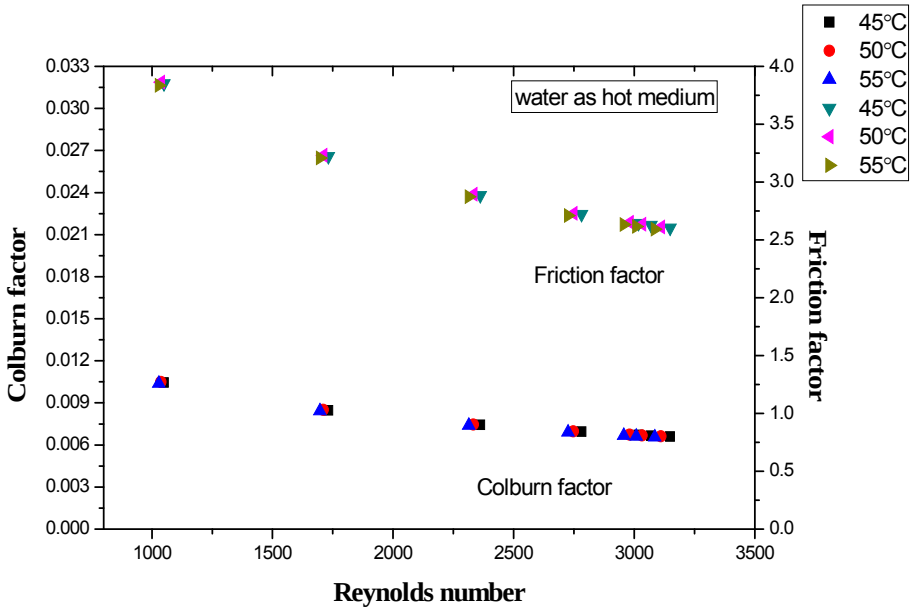

Fig. 5.2: Influence of Reynolds number on colburn factor and friction factor for air side.

Colburn factor of air decreases as the Reynolds number of air increases when nanofluid is flow inside the tube. Similar trend is observed when 0.1% concentration of nanofluid flow inside the tubes as shown in Fig. 5.3. Friction factor of air also decreases as the Reynolds number of air increases. Similar trend is observed in other case as shown in Fig. 5.4 for 0.2% concentration of nanofluid. Thinner boundary layer occurred at high velocity of air. Fin side heat transfer was studied by Colburn factor, which is dimensionless heat transfer coefficient and friction factor. . Multi louvered fins break the thermal boundary layer and increase the heat transfer rate.

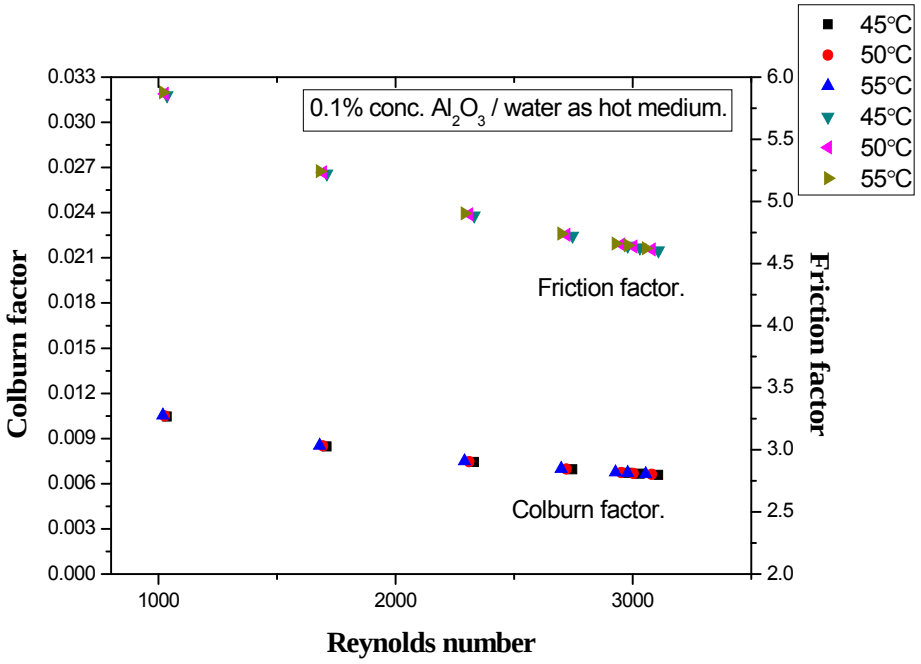

Fig 5.3: Influence of Reynolds number on colburn factor and friction factor for air side.

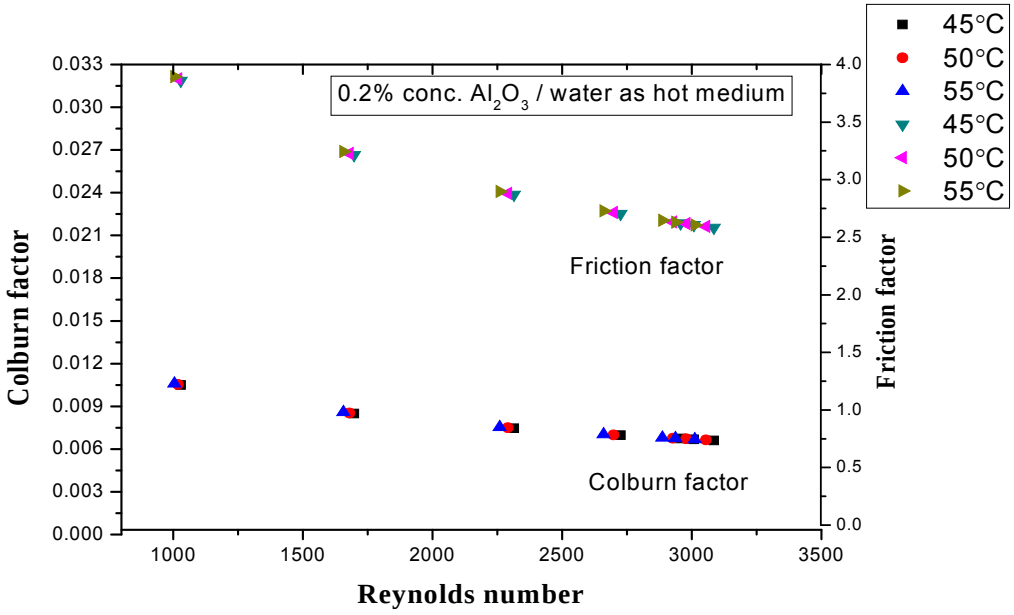

Fig. 5.4: Effect of Reynolds number on colburn factor and friction factor for air side.

As shown in Fig. 5.2 similar observation can be made when graph is plotted at all temperature and nanofluid concentration for colburn factor and friction factor of air. Colburn factor of air is decreases as the Reynolds number increases as shown in Fig. 5.5.

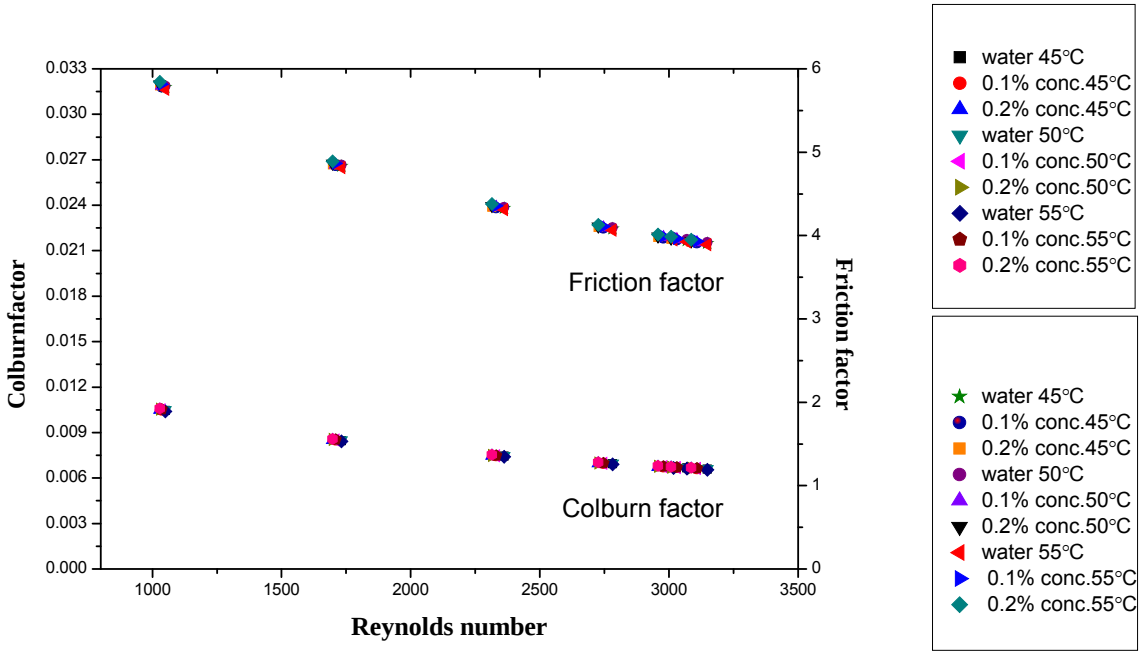

Fig. 5.5: Combined effect of Reynolds number on colburn factor and friction factor for air.

Nusselt number is represented as dimensionless temperature gradient at the surface. As the air side Reynolds number increased the Nusselt number value increased for a given inlet temperature as shown in Fig. 5.6.

As the inlet temperature of fluid inside the tube increased the value of Nusselt number decreased, because air viscosity increased and density decreased reason is that the surface temperature of tube increased, therefore Reynolds number of air decreased. Also, Nusselt number is function of Prandtl number. Prandtl number of air side decreased as temperature is increased from 20°C to 70°C. The value of Nusselt number for air side is function of both Reynolds number and Prandtl number. As the Reynolds number increased the value of Nusselt number increased at a given temperature as shown in Fig. 5.7. As the concentration of nanofluid increased the Nusselt number increased because thermal conductivity increased.

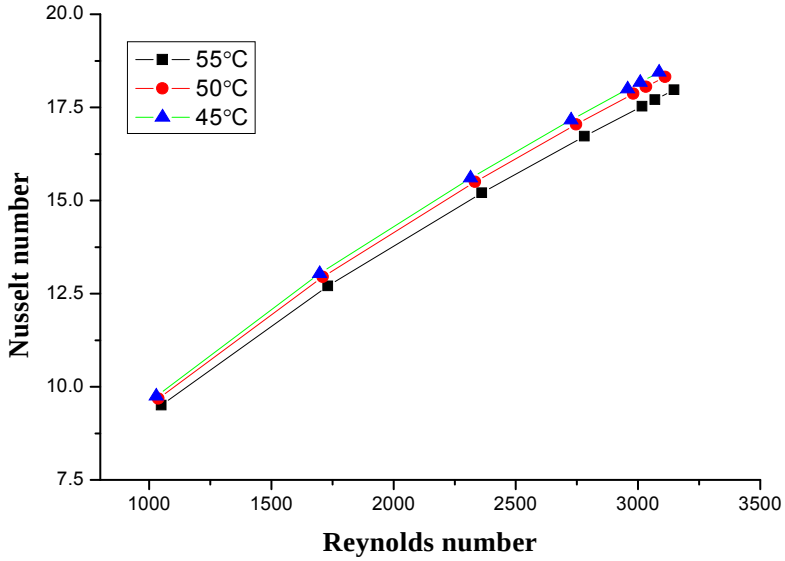

Fig. 5.6: Influence of Reynolds number on Nusselt number for air when water is hot medium inside tube.

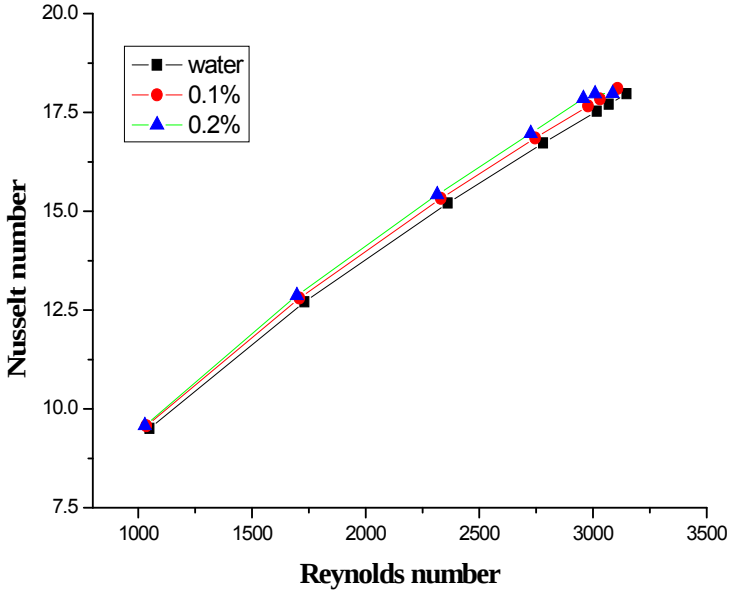

Fig. 5.7: Effect of Reynolds number on Nusselt number for air when inlet temperature of fluid in tube is 45°C.

As the hot fluid in tube side is changed and as the concentration of nanoparticles changed the value of Nusselt number of air is increased as the concentration of nanoparticles is increased, because thermal conductivity is increased, as shown in Fig. 5.8 and Fig. 5.9.

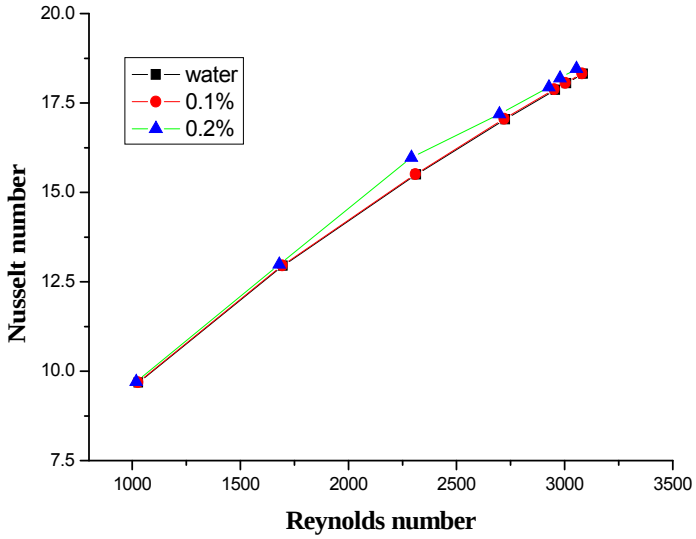

Fig. 5.8: Nusselt number vs. Reynolds number graph for air when fluid tube side at 50°C inlet temperature.

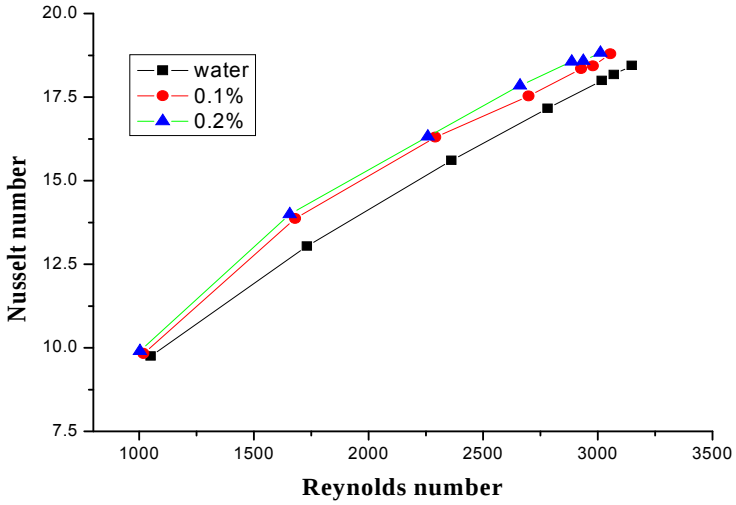

Fig. 5.9: Nusselt number vs. Reynolds number graph of air when fluid inside at 55°C temperature.

At 0.1% conc. of Al_2O_3 in water as shown in Fig. 5.10, the hot fluid at tube side at different temperatures, the value the Nusselt number of air increased as the value of inlet temperature decreased. Similar trend is observed by 0.2% conc. of Al_2O_3 in water as shown in Fig. 5.11.

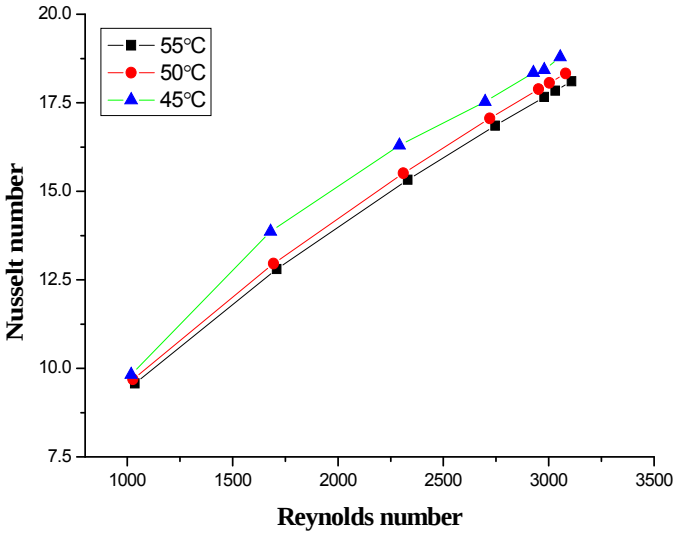

.

Fig. 5.10: Nusselt number vs. Reynolds number for air at 0.1% concentration of Al_2O_3 in water.

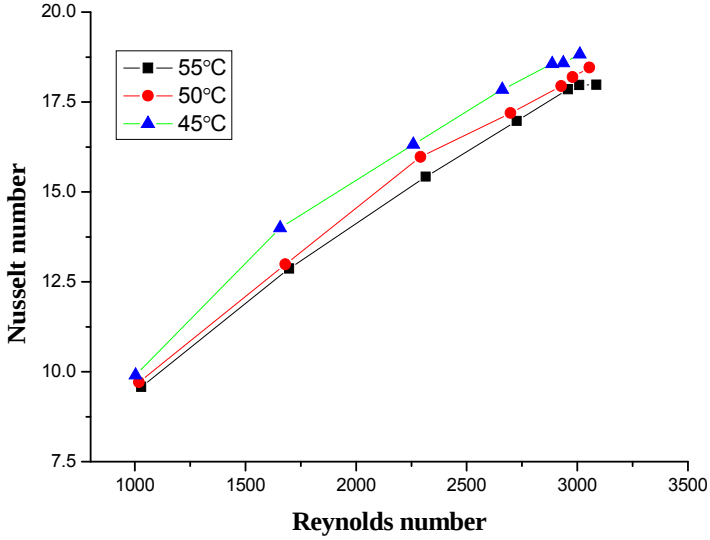

Fig. 5.11:- Nusselt number vs. Reynolds number of air at 0.2% conc. of Al_2O_3 in water.

5.2.2Tube side analysis

Experiments were done with water and nanofluid as working fluid at different inlet temperatures. Concentration of Al_2O_3 nanoparticles in nanofluid were 0.1% and 0.2% respectively in water. Nanoparticles increased the thermal conductivity of fluid flow inside the tube; therefore heat transfer rate increased. Friction factor is another important parameter of flowing fluid. Pressure drop and pumping power were determined by friction factor. As the concentration of nanoparticles increased, the base fluid viscosity and density increased and therefore must be increased in friction factor and pressure drop. Hence, nanofluids generally required the greater pumping power than their base fluid. It is also observed that by increasing the Reynolds number the pressure drop increased. Thermal performance of base fluid increased with increased in nanoparticle concentration without huge penalty in pumping power Tube side results are discussed below

The friction factor value decreased as the Reynolds number increased at the same temperature. But, as the temperature is increased the value of friction factor is decreased, because for liquids the viscosity is decreased as temperature of hot fluid in tube is increased as a result Reynolds number is increased as shown in Fig. 5.12.

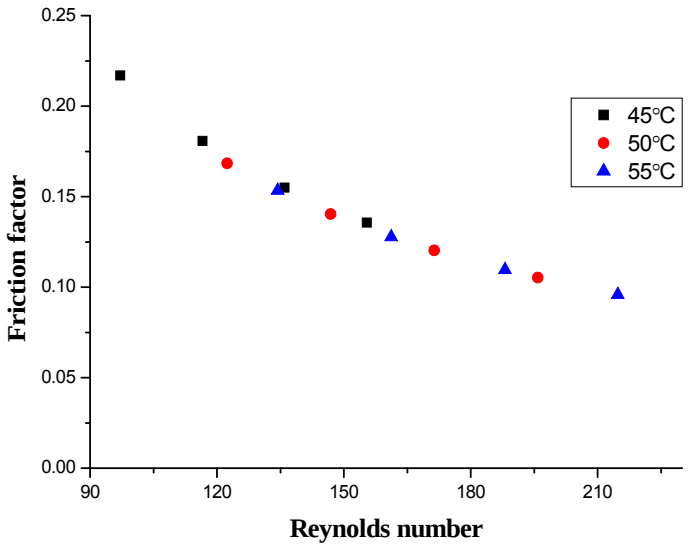

Fig. 5.12: - Friction factor vs. Reynolds number graph for water.

Similarly at the same concentration, as the temperature of nanofluid increased the value of Reynolds number increased and friction factor value decreased as shown in Fig. 5.12, because viscosity of nanofluid is decreases. Similar trend is observed by 0.1% concentration of nanofluid as shown in Fig. 5.13 below.

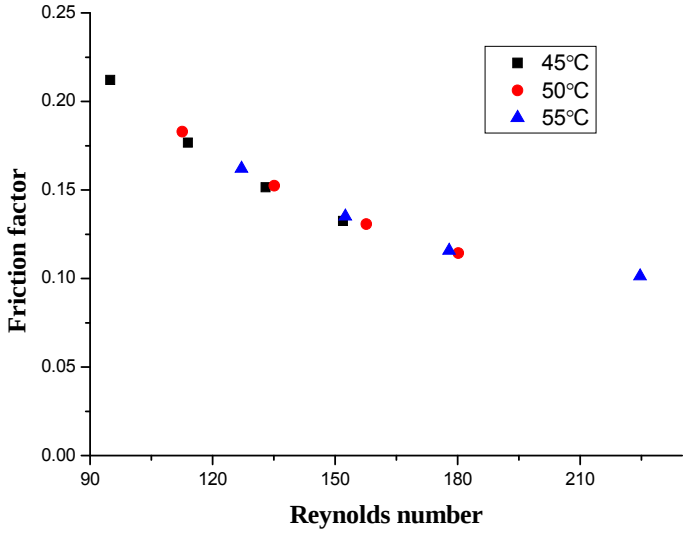

Fig. 5.13: - Friction factor vs. Reynolds number at 0.1% concentration of Al_2O_3 in water.

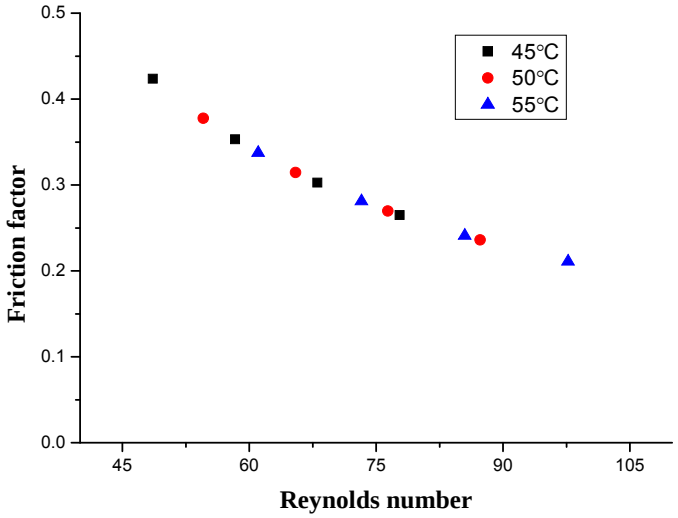

Fig. 5.14: - Friction factor vs. Reynolds number at 0.2% concentration of Al_2O_3 in water.

Nusselt number is function of both Reynolds number and Prandtl number. Its value depends upon both the dimensionless numbers, as the value of Reynolds number increased at a given temperature the Nusselt number increased as shown in Fig. 5.14 below. Because as the temperature of water increases the viscosity and density of water decreases, but effect of viscosity is predominant thus the value of Reynolds number increases, but at same time value of Prandtl number decreases, and as a combination of both Reynolds number and Prandtl number values Nusselt number increases.

Nusselt number in all concentration has increased by increase in the flow rate of fluid. The concentration of nanoparticles plays an important role in heat transfer. Whenever the concentration become greater, heat transfer become larger. Also increased in fluid inlet temperature slightly improves the heat transfer coefficient. Nusselt number behaviors of nanofluids highly depended on volume flow rate, inlet temperature and nanofluid volume concentration [2, 4].

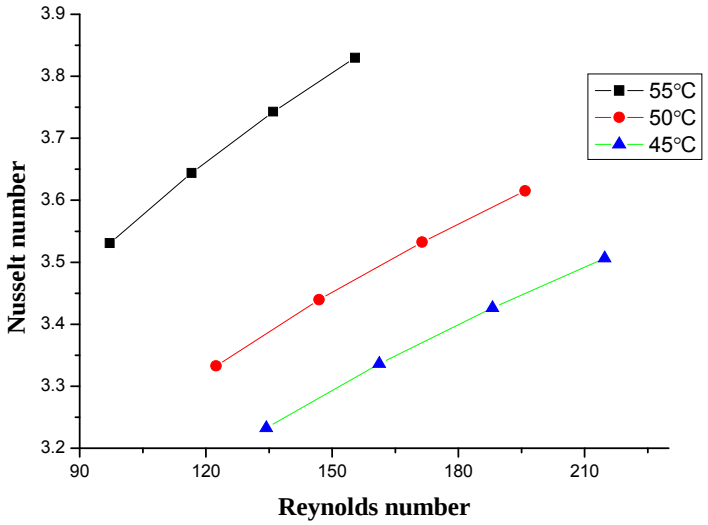

Fig. 5.15: Nusselt number vs. Reynolds number graph for water in tubes at different temperature.

Nusselt number increased as the value of Reynolds number increased as shown in Fig. 5.16, but as the inlet temperature of Nanofluid (at 0.1% concentration) increased, the viscosity of nanofluid decreased thus the value of Reynolds number increases. Previous researches suggested that the Brownian motion of nanoparticles and their random motion in base fluid increased the heat transfer rate. It caused thickness of thermal boundary layer to reduce and enhance the heat transfer. Similarly same trend was observed at 0.2% concentration of nanofluid as shown in Fig. 5.17.

It was considered that slip velocity mechanism occurred in nanofluids which produced a relative velocity between the nanoparticle and base fluid. Brownian diffusion (that is collision between nanoparticles and base fluid particles which transfer energy) occurred between the nanoparticles and base fluid particles, and both convection and conduction affect the Nusselt number [1, 2].

“Nusselt number at different temperature is analyzed the effect of temperature variation on the heat transfer performance of the cross flow heat exchanger. It is clear that Nusselt number increased as the inlet temperature increased. The variation of Nusselt number may be attributed to effect of temperature on thermo physical properties [5]”.

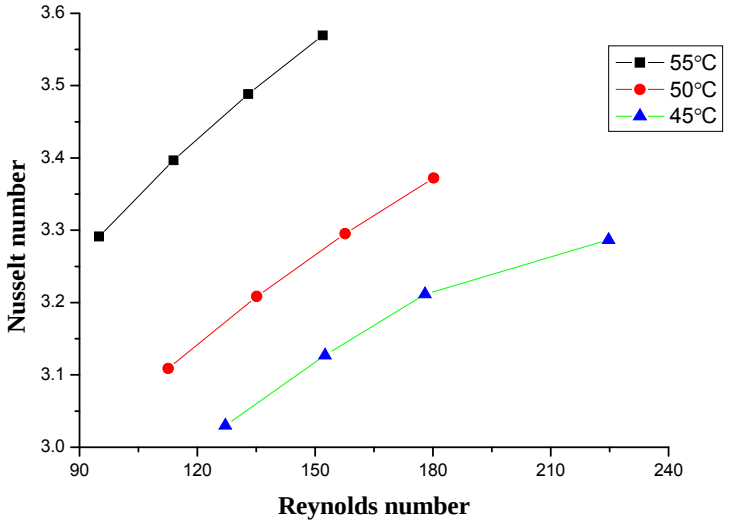

Fig. 5.16: Nusselt number vs. Reynolds number graph for 0.1% conc. of Al_2O_3 with water.

At 0.2% concentration Brownian motion of nanoparticles increased as the inlet temperature of the nanofluid increases. Number of particles a percentage increased which increased the random motion of particles. These random motions increase the convective and conductive heat gain. As a result Nusselt number increases as shown in Fig. 5.17.

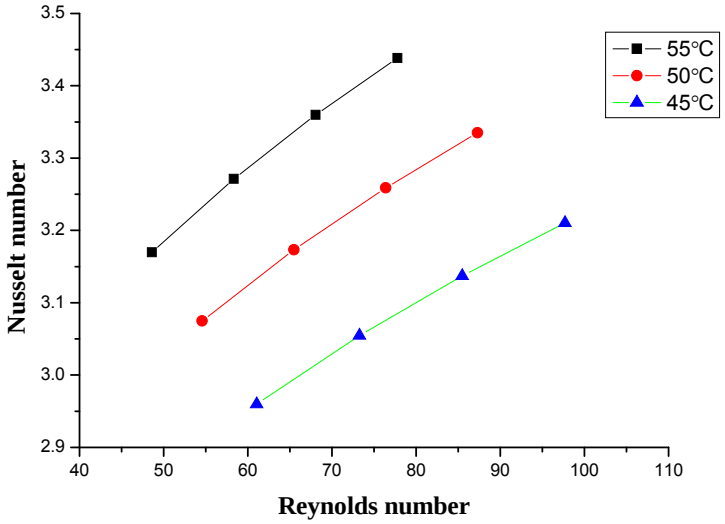

Fig. 5.17:- Nusselt number vs. Reynolds number graph for 0.2% conc. of Al_2O_3.

Colburn factor, Friction factor, and Nusselt number are discussed above for hot section. It is observed that nanofluid increased the heat transfer rate which depends upon the concentration of nanoparticles in base fluid. Brownian motion and slip velocity played important role in heat transfer enhancement. Thermal boundary layer has its own importance in heat transfer enhancement. Thinner the thermal boundary layer higher the heat transfer rate between the fins. Thinner boundary layer occurred at high velocity of air. Friction factor is increased as the flow over the fin is quite uniform. Nusselt number increased as the concentration increased because of increased in thermal conductivity of fluid flow inside the heat exchanger.

5.3 Cold section heat transfer and fluid flow characteristics.

5.3.1 Fin (Air) side Analysis

As the air side Reynolds number increased the Nusselt number value increased for given inlet temperature as shown in Fig. 5.18. As the inlet temperature of fluid inside the tube increased the value of Nusselt number decreased, because air viscosity increased and density decreased reason is that the surface temperature of tube increases as the inlet temperature of fluid increases, therefore Reynolds number of air decreases.

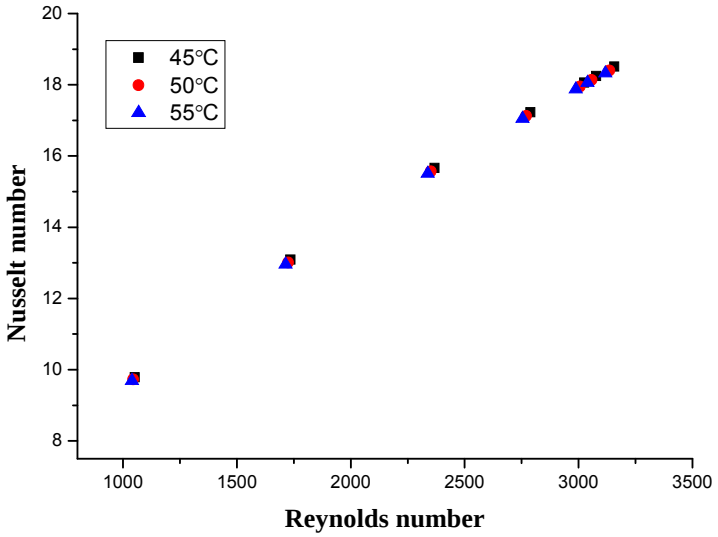

Fig. 5.18: Nusselt number vs. Reynolds number graph of air for water at different inlet temperatures.

At 0.1% conc. of Al_2O_3 in water for different temperatures the value of Nusselt number increased as the value of Reynolds number increased at a given inlet temperature. The value the Nusselt number of air increased as the value of inlet temperature decreased. There is very small difference in values because the temperature difference in cold section is small as compare to hot section. Therefore the data points are very close to each other.

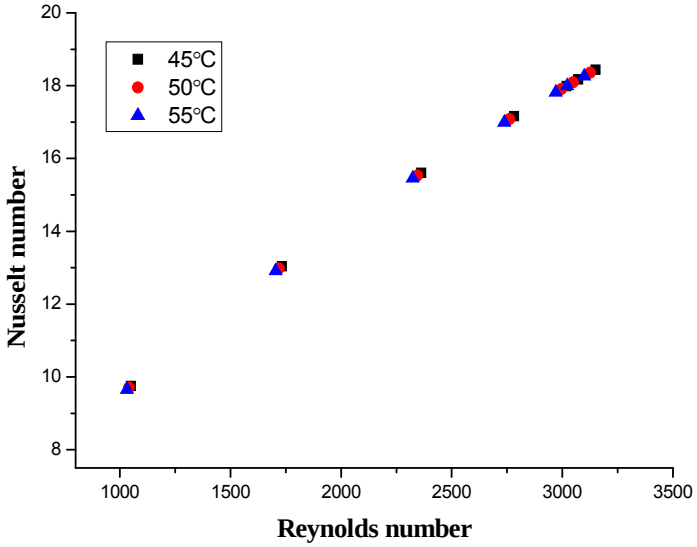

Fig. 5.19: Nusselt number vs. Reynolds number of air at 0.1% conc. of Al_2O_3 in water.

Similarly the same effect is seen as shown in Fig. 5.19 when concentration of nanofluid is changed from 0.1% to 0.2%. Difference in decrement is small but clearly seen in Fig 5.20 as shown below.

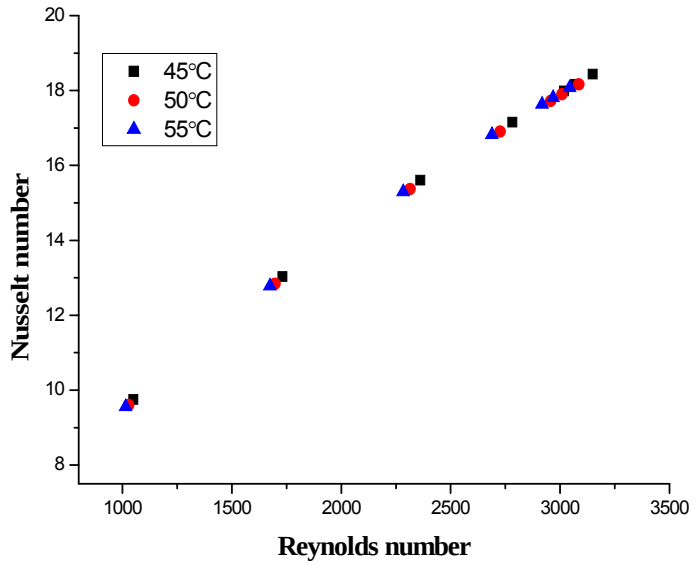

Fig. 5.20: Nusselt number vs. Reynolds number of air at 0.2% conc. of Al_2O_3 in water.

At 45°C inlet temperature for different concentrations of nanoparticle the value of Nusselt number increased as the Reynolds number value increased. As the concentration of nanoparticles changed the value of Nusselt number of air is increased as the concentration of nanoparticles is increased, because thermal conductivity is increased which increase the heat transfer as shown in Fig. 5.21.

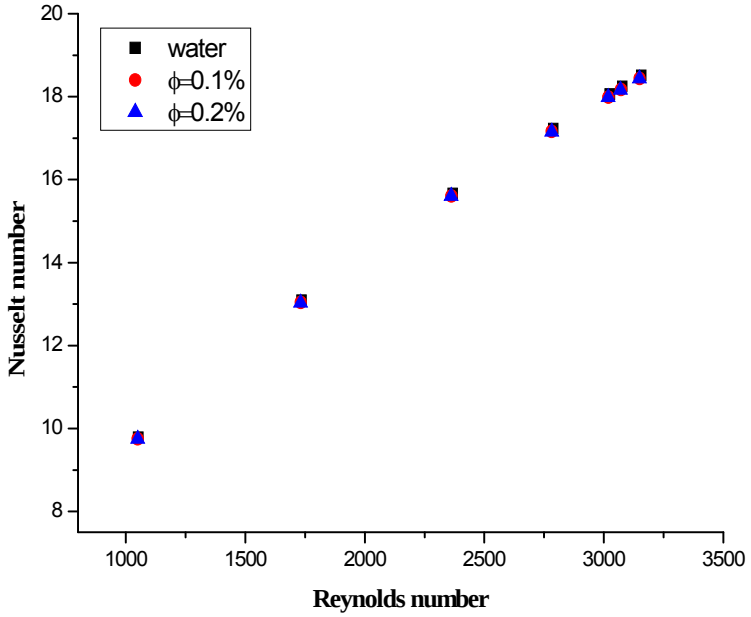

Fig.5.21: Nusselt number vs. Reynolds number graph of air at 45°C temperature.

Similarly as the inlet temperature of hot fluid in tubes is increased to 50°C and 55°C similar trend is observed in Fig. 5.22 and Fig 5.23. As the concentration of nanofluid increased the conduction heat transfer increases as a result the Nusselt number increased. Rise in Nusselt number is very small over water when nanofluid is flowing in tubes.

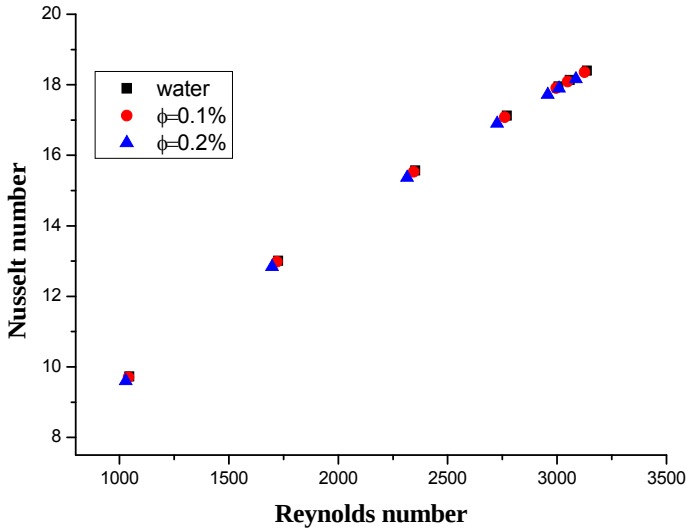

Fig. 5.22: Nusselt number vs. Reynolds number graph of air at 50°C temperature.

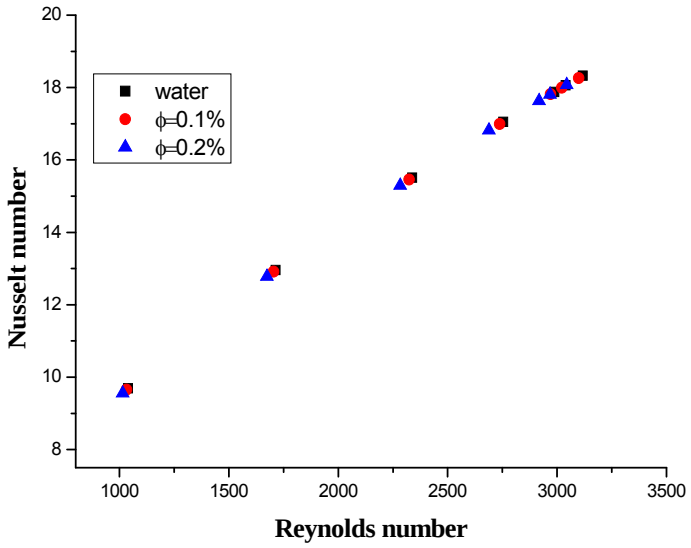

Fig. 5.23: Nusselt number vs. Reynolds number graph of air at 55°C temperature.

Colburn factor of air decreased as the value of Reynolds number increases, because Stanton number decreases as the Reynolds number increases. The value of Prandtl number of air decreased as the temperature of air increased from 25°C to 75°C. Whereas Friction factor of air as shown in Fig. 5. 24 also decreased as the value of Reynolds number increases. As the

flow is as more as louvered directed the friction factor is high. As the temperature increases the value of Colburn factor and friction factor increases.

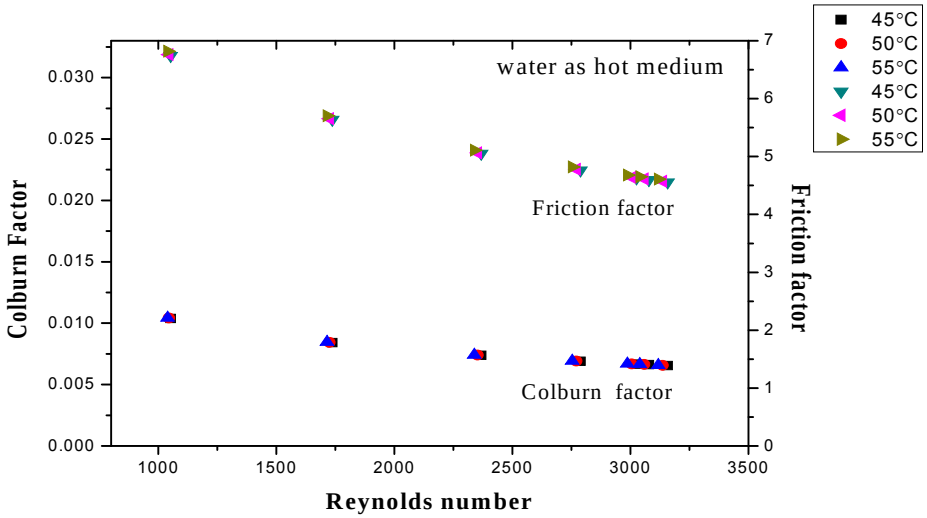

Fig. 5.24: Influence of Reynolds number on Colburn factor and friction factor of air.

Colburn factor of air decreases as Reynolds number increases, when nanofluid is flow inside the tube as shown in Fig. 5.25. Similar trend is observed for friction factor.

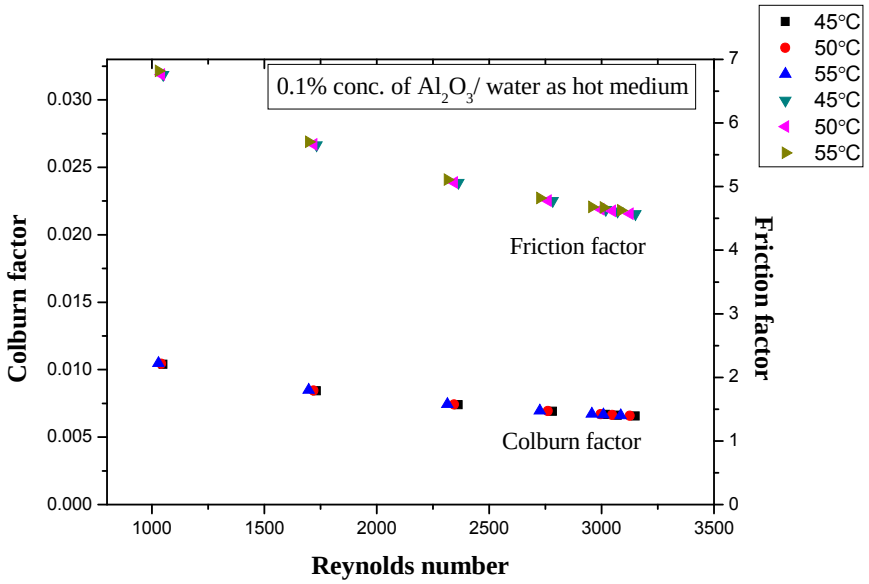

Fig. 5.25: Influence of Reynolds number on Colburn factor and friction factor of air.

Similarly same trend was observed when the concentration of nanofluid is changed from 0.1% to 0.2%. As the temperature of nanofluid increased the value of colburn factor increased as shown in Fig. 5.26. As the value of temperature increased the Colburn factor and friction factor increased.

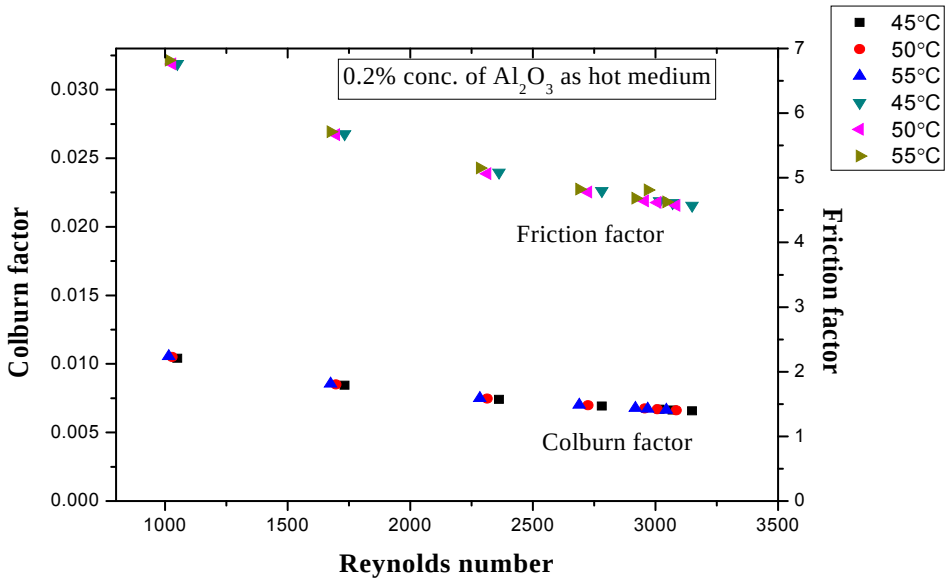

Fig. 5.26: Effect of Reynolds number on Colburn factor and friction factor of air.

5.3.2 Tubes side analysis.

For cold section fluid moved from bottom collecting tank to header of cross flow heat exchanger. Heat is gained by fluid when it rises from bottom to up. Nanofluid is used at measuring concentrations which increased the heat transfer rate. Thermal conductivity of nanoparticles played very important role here. Friction factor and Reynolds number are two important parameters for fluid flow characteristics are discussed below.

Friction factor of water decreased as the Reynolds number increases at a given temperature but as the temperature is increased the value of friction factor is decreased because for liquids Reynolds number increases as result of decrease in viscosity as shown in Fig. 5.27 below

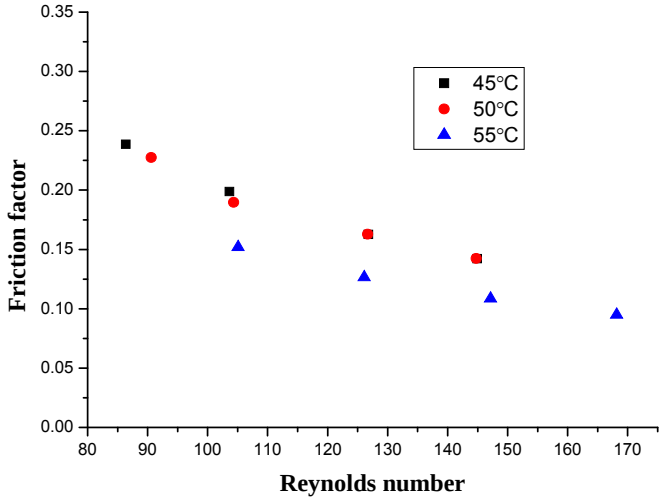

Fig. 5.27: Friction factor vs. Reynolds number graph for water at different inlet temperatures.

At 0.1% concentration, friction factor decreased as the value of Reynolds number increased as shown in Fig. 5.28, because friction factor is inversely depends upon the Reynolds number. As the value of temperature increased at same concentration, friction factor value decreased because viscosity decreased and Reynolds number value increased.

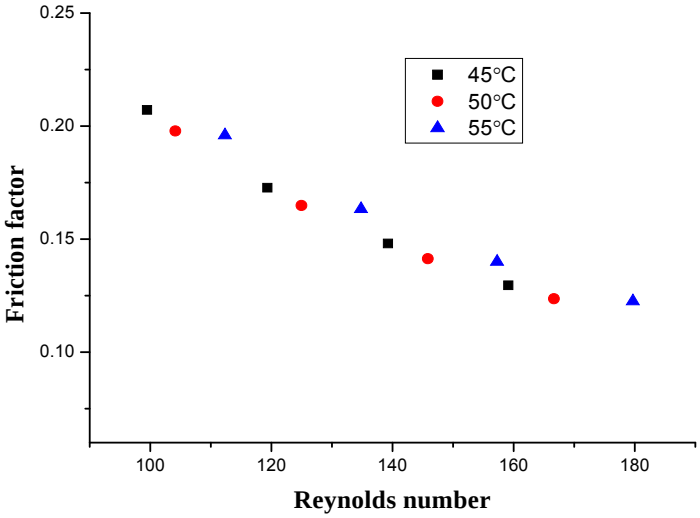

Fig. 5.28: Friction factor vs. Reynolds number graph for tube side at 0.1% conc. of nanofluid.

Friction factor value as shown in Fig. 5.29 decreased as the value of Reynolds number increased but as the concentration of nanoparticles increased in water the value of friction factor is increased as the viscosity of nanofluid increased. Similar trend is observed at 55°C temperature various concentrations as shown below in Fig. 5.30.

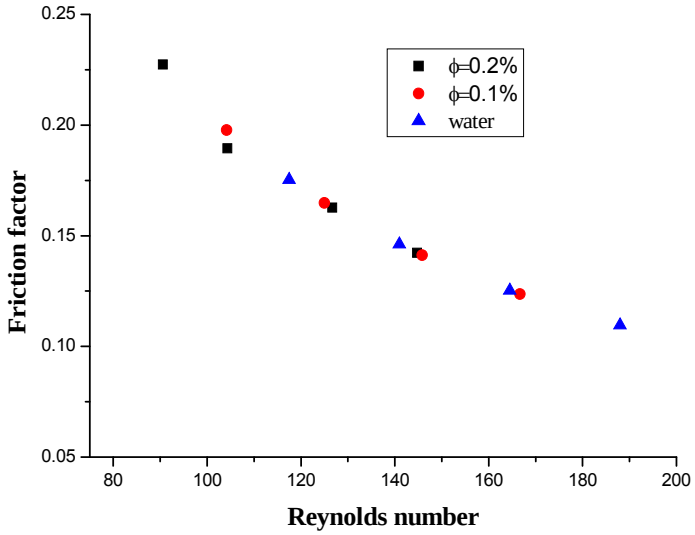

Fig. 5.29: Friction factor vs. Reynolds number for tube side flow at 50°C temperature for different conc. of nanoparticles.

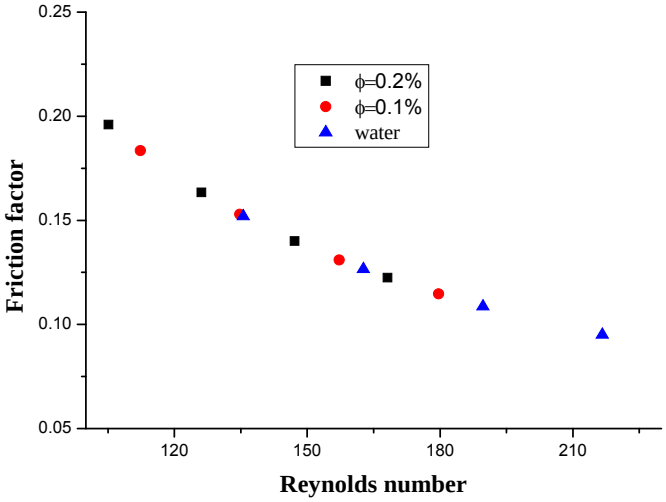

Fig. 5.30:-Friction factor vs. Reynolds number tube side flow at 55°C temperature.

Nusselt number increased as the value of Reynolds number increased. But as the temperature of nanofluid at 0.2% concentration increased, the heat transfer coefficient improves slightly. Also viscosity of nanofluid decreased thus the value of Reynolds number increased, and Nusselt number increased as shown in Fig. 5.31.

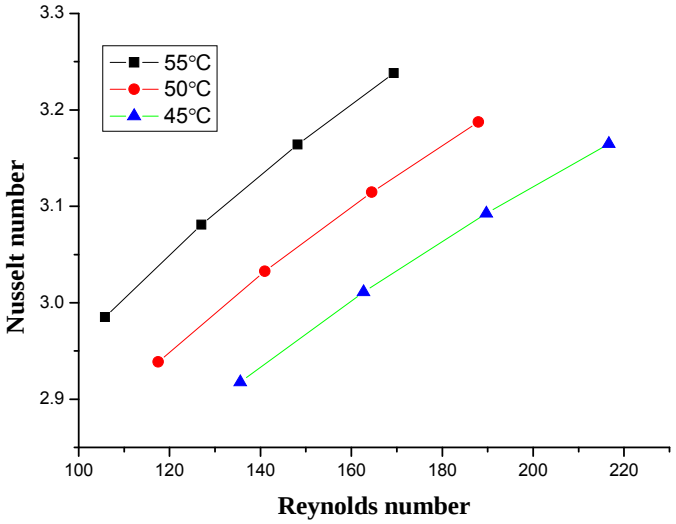

Fig. 5.31: Nusselt number vs. Reynolds number graph for 0.2% conc. of Al_2O_3 at different temperature.

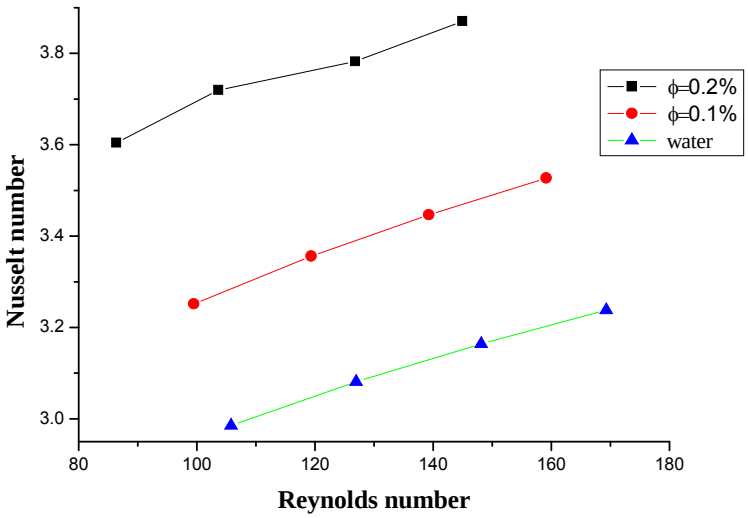

Fig. 5.32: Nusselt number vs. Reynolds number for tube side fluid at 45°C inlet temperature.

At same temperature as the concentration of nanoparticle increased the value of heat transfer coefficient become larger as a result Nusselt number increased [2] as shown in Fig. 5. 32. Similar trend is observed at 50°C and 55°C as shown below in Fig. 5.33 and Fig. 5.34 respectively.

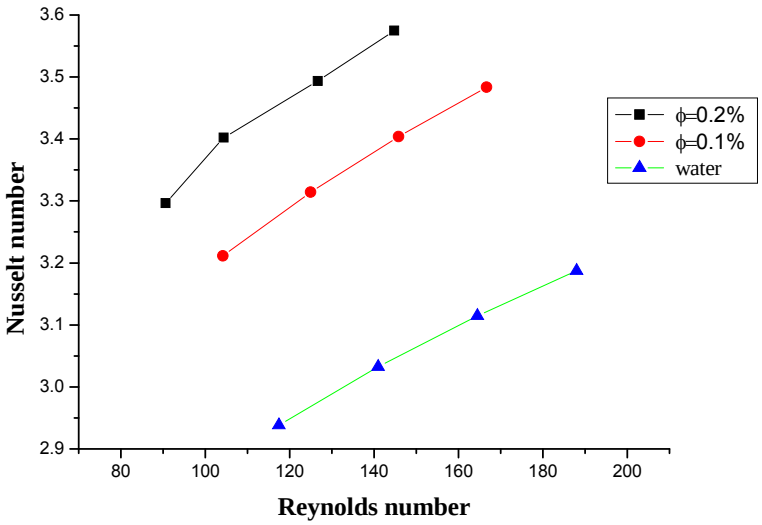

Fig. 5.33:- Nusselt number vs. Reynolds number for tube side fluid at 50°C inlet temperature.

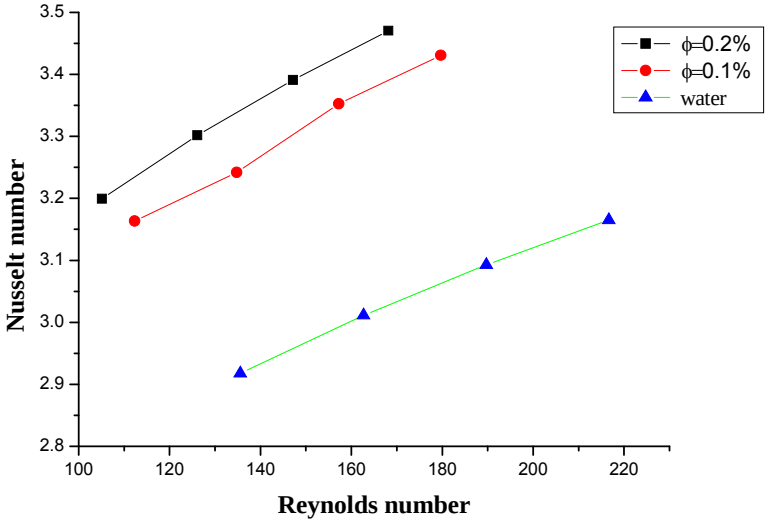

Fig. 5.34:- Nusselt number vs. Reynolds number for tube side fluid at 55°C inlet temperature.

5.4 Regression analysis

Correlation of Colburn factor with Reynolds number at 45°C temperature.

Correlations of the *j* factor were obtained by experimental values from copper-brass cross flow multi louvered fin compact heat exchanger. The main focus of this regression analysis and F significance test is to observe the relation between colburn factor and Reynolds number.

$$J_a = C_1 \times Re_a^b \quad (5.1)$$

Where C_1 and *b* are curve fit coefficient. And values are given in table 5.1 below. Regression is done with all data points fitted with power law as given in equation 5.1. (R^2 value) the coefficient of determination for each equation is given in table 5.1a, 5.2, and 5.3 respectively.

$$J_a = 0.1930 \times Re_a^{-0.42} \quad (5.1a)$$

Similarly colburn factor relation with Reynolds number at 50°C and 55°C temperature. Is given below

$$J_a = C_2 \times Re_a^d \quad (5.2)$$

Where C_2 and *d* are curve fit coefficient. And values are given in table 5.2 below

$$J_a = 0.1937 \times Re_a^{-0.42}$$

(5.2a)

$$J_a = C_3 \times Re_a^e \quad (5.3)$$

Where C_3 and *e* are curve fit coefficient. And values are given in table 5.3 below

$$J_a = 0.1930 \times Re_a^{-0.42} \quad (5.3a)$$

Table 5.1: Regression summary between colburn factor and Reynolds number for 45°C temperature.

SUMMARY OUTPUT FOR 45°C TEMPERATURE

Regression Statistics	
Multiple R	0.95077
R Square	0.95077
Adjusted R Square	0.95073
Standard Error	3.073E-16
Observations	7

ANOVA

	df	*SS*	*MS*	*F*	*Significance F*
Regression	2	0.032888388	0.01644	1.741E+29	1.32E-58
Residual	4	3.77806E-31	9.4E-32		
Total	6	0.032888388			

	Coefficients	*Standard Error*	*t Stat*	*P-value*	*Lower 95%*	*Upper 95%*	*Lower 95.0%*	*Upper 95.0%*
Intercept	-0.7128289	3.17826E-11	-2.2E+10	2.3712E-41	-0.7128289	-0.7128289	-0.71282887	-0.71282887
X Variable 1	-0.42	1.77069E-15	-2.4E+14	1.8955E-57	-0.42	-0.42	-0.42	-0.42

Table 5.2: Regression summary between colburn factor and Reynolds number for 50°C temperature.

SUMMARY OUTPUT OF 50°C TEMPERATURE

Regression Statistics	
Multiple R	0.95081
R Square	0.95081
Adjusted R Square	0.95077
Standard Error	2.99092E-16
Observations	7

ANOVA

	Df	*SS*	*MS*	*F*	*Significance F*
Regression	2	0.032888388	0.01644419	1.8382E+29	1.18373E-58
Residual	4	3.57824E-31	8.9456E-32		
Total	6	0.032888388			

	Coefficients	*Standard Error*	*t Stat*	*P-value*	*Lower 95%*	*Upper 95%*	*Lower 95.0%*	*Upper 95.0%*
Intercept	-0.712828871	7.23937E-13	-9.847E+11	6.3828E-48	-0.712828871	-0.71282887	-0.71282887	-0.71282887
X Variable 1	-0.42	1.45501E-15	-2.887E+14	8.6422E-58	-0.42	-0.42	-0.42	-0.42

Table 5.3: Regression summary between colburn factor and Reynolds number for 55°C temperature.

SUMMARY OUTPUT FOR 55°C TEMPERATURE.

Regression Statistics	
Multiple R	0.95097
R Square	0.95097
Adjusted R Square	0.95089
Standard Error	1.27E-16
Observations	7

ANOVA

	Df	*SS*	*MS*	*F*	*Significance F*
Regression	2	0.032888	0.016444	1.01E+30	3.89E-60
Residual	4	6.49E-32	1.62E-32		
Total	6	0.032888			

	Coefficients	*Standard Error*	*t Stat*	*P-value*	*Lower 95%*	*Upper 95%*	*Lower 95.0%*	*Upper 95.0%*
Intercept	-0.7143	9.6E-13	-7.4E+11	1.96E-47	-0.7143	-0.7143	-0.7143	-0.7143
X Variable 1	-0.42	6.76E-16	-6.2E+14	4.02E-59	-0.42	-0.42	-0.42	-0.42

References

[1] Huminic G., Huminic A., (2013), “Numerical analysis of laminar flow heat transfer of nanofluid in flattened tube” , International Communication in Heat and Mass Transfer Vol. 44, 52-57.

[2] Peyghambarzadeh S.M., Hashemabadi S.H., Hoseini S.M., Seifi Jamnani M., (2011), “Improving the cooling performance of automobile radiator with Al_2O_3/water nanofluid”, Applied Thermal Engineering Vol. 31, 1833-1838.

[3] Li Wei, Wang Xialing., (2010). “ Heat transfer and pressure drop correlation for compact heat exchangers with multi-regioon louver fins”, International Communication in Heat and Mass Transfer Vol. 53, 2955-2962.

[4] Hussein Adnan M., Bakar R.A., Kadirgama K., Sharma K.V., (2014), “Heat transfer enhancement using nanofluids in an automotive cooling system”, International Communications in Heat and Mass Transfer Vol. 53, 195–202.

[5] Peyghambarzadeh S.M., Hashemabadi S.H., Hoseini S.M., Seifi Jamnani M., (2011), “Experimental study of heat transfer enhancement using water/ethylene glycol based nanofluids as a new coolant for car radiators”, International Communications in Heat and Mass Transfer Vol. 38, 1283–1290.

Chapter-6

Conclusion

Experimental work had been done on cross flow heat exchanger which having U type flow in tubes. Nanofluids were prepared with Al_2O_3 nanoparticles in distilled water as base fluid at 0.1% and 0.2% concentration. The experiments were conducted at 45°C, 50°C, and 55°C temperature, with four flow rates 25, 30, 35, and 40 LPH respectively.

Hot section of cross flow heat exchanger

- For air, Nusselt number for 0.1% concentration (of nanofluid as hot fluid) enhanced by 1% to 1.1% with respect to at 45°C temperature for hot section side.
- As the temperature of nanofluid at 0.1% concentration was increased to 50°C and 55°C, the heat transfer coefficient was increased by 5.94%, 11.57% respectively with respect to water.
- There was 16.38% and 18.51% enhancement of heat transfer coefficient with respect to water at 50°C and 55°C temperature, when 0.2% concentration of nanofluid is taken as hot fluid at tube side.
- Effectiveness of cross flow heat exchanger was also increased. It was 68.52% for distilled water, and increased to 72.56% and 74.21% for 0.1% and 0.2% concentration of Al_2O_3 in water, respectively.
- Tube side friction factor increases with concentration of nanoparticles; enhancement was observed 11.11% at 45°C temperature with respect to water for 0.1% concentration of nanofluid, and 25.56% enhancement with respect to water for 0.2 % concentration of nanofluid.
- As temperature of hot fluid increased to 50°C and 55°C, friction factor of nanofluids at 0.1% concentration and 0.2% concentration was increased by 8.73% and 16.37% with respect to water respectively.

Cold section of heat exchanger

Cold section having less difference in temperature as compare to hot section when fluid flow upward from bottom collecting tank to outlet of heat exchanger. As discussed earlier heat is gained by the fluid in cold section as it moves in upward direction. Therefore very small enhancement is observed. As discussed below.

- For air, Nusselt number for 0.1% concentration (of nanofluid as hot fluid) enhanced by 0.5% to 0.7% with respect to at 45°C temperature for cold section side.
- As the temperature of nanofluid at 0.1% concentration was increased to 50°C and 55°C, the heat transfer coefficient was increased by 1.53%, 3.46% respectively with respect to water.
- There was 2.50% and 4.78% enhancement of heat transfer coefficient with respect to water at 50°C and 55°C temperature, when 0.2% concentration of nanofluid is taken as hot fluid at tube side.
- Effectiveness of cross flow heat exchanger was also increased. It was 39.2% for distilled water, and increased to 48.96% and 56.78% for 0.1% and 0.2% concentration of Al_2O_3 in water, respectively.
- Tube side friction factor increases as the concentration of nanoparticles enhancement was observed 12.49% at 45°C inlet temperature with respect to water for 0.1% concentration of nanofluid, and 17.72% enhancement with respect to water for 0.2 % concentration of nanofluid.
- As inlet temperature of hot water increased to 50°C and 55°C, friction factor of nanofluids at 0.1% concentration and 0.2% concentration was increased by 9.27% and 14.37% with respect to water respectively.

Chapter-7

Future scope of work

- Experiment can be done by taking different particle size for Al_2O_3 with different concentration of nanoparticle in base fluid.
- Different nanoparticles can be taken with different concentration.
- Base fluid can be changed with different types of nanoparticles with different concentration.
- After cooler can be used with heat exchanger to enhance the cooling effect.
- CFD analysis can be done and results will compare with experimental work.
- Study the performance of heat exchanger when couple with engine cooling system.

Annexure

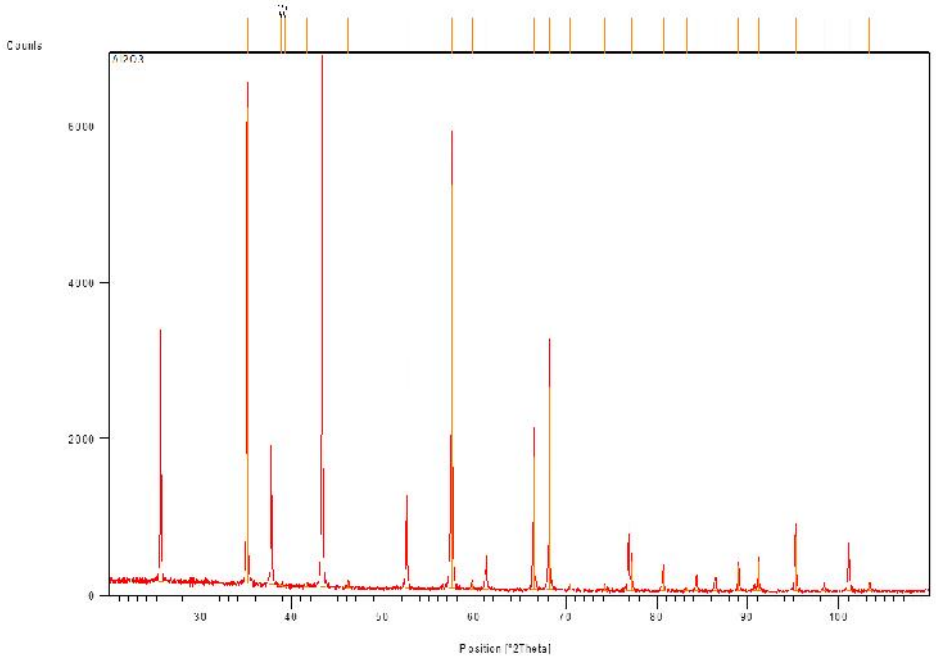

Fig. A1: XRD image of Al_2O_3 nanoparticles

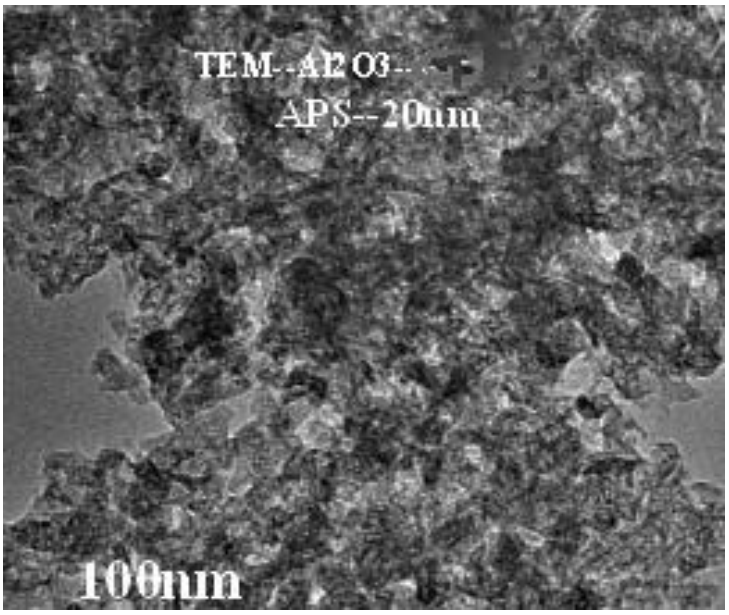

Fig. A2: TEM image of Al_2O_3 nanoparticles

Table A1: Thermal conductivity of Al_2O_3 at 0.1% concentration

CONCENTRATION 0.1%	
TEMPERATURE (ºC)	THERMAL CONDUCTIVITY (W/mK)
31.25	0.621
31.5	0.623
32.5	0.629
33.52	0.633
34.2	0.639
36.92	0.642
37.8	0.645
39.3	0.647
42.3	0.669
44.3	0.674
50.3	0.686
55.2	0.723
60.23	0.758
66.2	0.793
69.32	0.831
70.42	0.856
75.42	0.903
80.2	0.922

Table A2: Thermal conductivity of Al_2O_3 at 0.2% concentration

CONCENTRATION 0.2%	
TEMPERATURE (ºC)	THERMAL CONDUCTIVITY (W/mK)
31.25	0.629
32.5	0.635
33.37	0.64
35.23	0.646
38.51	0.656
39.3	0.664
42.8	0.673
45.25	0.709
50.35	0.753
55.75	0.768
60.25	0.863
65.4	0.912
70.5	0.937
76.43	0.987
80.23	1.24

Table A3: Viscosity of Al_2O_3 at 0.1% concentration

CONCENTRATION 0.1%	
TEMPERATURE (ºC)	VISCOSITY (cP)
30	0.72
40	0.59
50	0.48
60	0.35
70	0.27
80	0.19
30	0.72
40	0.59
50	0.48

Table A4: Viscosity of Al_2O_3 at 0.2% concentration

CONCENTRATION 0.2%	
TEMPERATURE (ºC)	VISCOSITY (cP)
30	0.68
40	0.52
50	0.4
60	0.31
70	0.22
80	0.16
30	0.68
40	0.52
50	0.4

Table A5: Density of water and Al_2O_3 at 0.1%, and 0.2% concentration respectively at different temperature

S.No.	TEMPERATURE(^oC)	WATER	0.1%	0.2%
1	25	986.8	1042.2	1048.3
2	35	983.0	1040.0	1044.0
3	40	980.6	1038.6	1041.4
4	45	975.0	1036.8	1038.2
5	50	973.4	1034.8	1037.0
6	55	972.0	1031.2	1033.5
7	60	971.2	1027.6	1030.1
8	70	968.8	1024.0	1026.4

Table A6: Showing readings of distilled water at 45°C temperature when velocity of air was 3.30 m/sec and water flow rate was 25LPH.

T1	T2	T3	T4	T5	T6	T7	T8	T9	T10
24	24	23.4	35.6	34.8	43.2	23.6	24	24	24.1
23.5	22.9	23.1	35.4	34	43.5	23	23.2	23.4	23
23.7	23.2	23.4	35.5	33.3	43.4	23.3	23.6	23.7	23.3
23.5	23.2	23.4	35.4	33.3	43.5	23.3	23.6	23.7	23.3
24	23.9	24	35.5	35.9	43.6	24.2	24	24.3	24.1
24	23.9	24	35.6	35.3	43.7	24.2	24	24.6	24.3
24.2	24.1	24.2	35.6	36.1	43.7	24.4	24.2	24.6	24.6
24.2	24.4	24.4	35.6	35.7	43.7	24.6	24.2	24.6	24.6
24.2	24	23.4	35.6	34.8	43.7	23.6	24.2	24.6	24.6

Table A7: Showing readings of distilled water at 45°C temperature when velocity of air was 6.00 m/sec and water flow rate was 25LPH.

T1	T2	T3	T4	T5	T6	T7	T8	T9	T10
24	24	23.4	36.8	35.1	43.5	23.6	24	24.3	24.6
24.6	22.9	23.1	36.4	35	43.7	23	23.2	24.4	24.6
24.5	23.2	23.4	36.5	35.3	43.8	23.3	23.6	24.4	24.8
24.5	23.2	23.4	36.4	35.3	43.8	23.3	23.6	24.5	24.8
24.4	24.9	24	36.5	35.3	43.7	24.7	24	24.3	24.7
24.4	24.9	24	36.6	35.3	43.8	24.8	24	24.5	24.7
24.4	25.1	24.2	36.7	36.7	43.8	25.1	24.2	24.5	24.6
24.4	25.4	24.4	36.7	36.7	43.8	25.4	24.2	24.5	24.6
24.4	25.4	23.4	36.7	36.7	43.8	25.4	24.2	24.5	24.6

Table A8: Showing readings of distilled water at 50°C temperature when velocity of air was 3.30 m/sec and water flow rate was 25LPH.

T1	T2	T3	T4	T5	T6	T7	T8	T9	T10
24.1	29	23.4	39.6	35.8	47.2	29.1	24	24	24.1
24.3	29.9	23.1	39.4	36	47.5	30	24.2	24.4	24.6
24.5	30.2	23.4	39.5	36.3	47.4	30.3	24.6	24.7	24.9
24.5	31.2	23.4	39.4	36.3	47.5	31.3	24.6	24.7	24.9
24.7	33.9	24	39.5	36.9	47.6	33.6	24.6	24.8	24.9
24.7	33.9	24	39.6	37.3	47.7	33.6	24.6	24.6	24.9
24.7	34.4	24.2	39.6	37.1	47.7	34.4	24.6	24.6	24.9
24.7	34.4	24.4	39.6	37.1	47.7	34.6	24.6	24.6	24.9
24.7	34.4	23.4	39.6	37.1	47.7	34.6	24.6	24.6	24.9

Table A9: Showing readings of distilled water at 50°C temperature when velocity of air was 6.00 m/sec and water flow rate was 25LPH.

T1	T2	T3	T4	T5	T6	T7	T8	T9	T10
24.1	29.6	23.4	39.9	35.8	47.7	29.1	24	24	24.1
24.3	30.9	23.1	39.9	36	47.7	30	24.2	24.4	24.6
24.5	31.2	23.4	39.9	36.3	47.7	30.3	24.6	24.7	24.9
24.5	31.2	23.4	39.9	36.3	47.9	31.3	24.6	24.7	24.9
24.7	33.8	24	39.5	36.9	47.9	33.6	24.6	25.	24.9
24.7	33.9	24	39.6	37.3	48.1	33.6	24.6	25.1	25
24.7	34.8	24.2	39.9	37.1	48.1	34.4	24.6	25.1	25
24.7	34.8	24.4	39.9	37.1	48.1	34.6	24.6	25.2	25
24.7	34.8	23.4	39.9	37.1	48.1	34.6	24.6	25.1	25

Table A10: Showing readings of distilled water at 55°C temperature when velocity of air was 3.30 m/sec and water flow rate was 25LPH.

T1	T2	T3	T4	T5	T6	T7	T8	T9	T10
22.7	22.4	36.9	45.3	23.5	54.5	22.5	22.8	22.9	23.1
22.7	22.2	33.3	45.3	23.5	54.6	22.4	22.8	22.9	22.9
22.7	22.4	34.9	45.3	23.5	54.7	22.5	22.9	23	22.9
22.5	22.4	35.2	45.3	23.5	54.7	22.5	22.8	23	23
22.7	22.3	34.8	45.3	23.5	54.7	22.5	22.8	22.9	23
22.7	22.3	35	45.3	23.5	54.8	22.5	22.8	22.9	23.1
22.7	22.3	36.9	45.3	23.5	54.8	22.4	22.8	22.9	23.1
22.7	22.3	36.9	45.3	23.5	54.8	22.4	22.8	22..9	23.1
22.7	22.4	36.9	45.3	23.5	54.8	22.5	22.8	22.9	23.1

Table A11: Showing readings of distilled water at 55°C temperature when velocity of air was 6.00 m/sec and water flow rate was 25LPH.

T1	T2	T3	T4	T5	T6	T7	T8	T9	T10
24	27	36.1	44.2	25.3	53.5	27.1	25.2	25.5	26.4
23.5	26.4	36.3	45.1	25.2	53.6	26.2	25.4	25.6	26
23.7	25.4	38.6	45.5	25.1	53.5	25.9	25.1	25.4	25.7
23.5	25.2	38.7	45	25	53.7	25.8	25	25.1	25.5
24	25.2	38.8	44.2	24.8	53.6	25.8	24.9	25	25.3
24	25.1	38.8	44.2	24.7	53.7	25.7	24.9	25	25.2
24.2	25.3	38.7	44.2	24.8	53.6	25.8	24.8	25	25.3
24.2	25.3	38.8	44.2	24.9	53.6	25.8	24.9	25.1	25.4
24.2	25.3	38.8	44.2	24.9	53.6	25.8	25.2	25.1	25.4

Table A12: Showing readings of Al_2O_3, 0.1 % concentration at 45°C temperature when velocity of air was 3.30 m/sec and water flow rate was 25LPH.

T1	T2	T3	T4	T5	T6	T7	T8	T9	T10
26.7	26.2	26.5	33.7	33.1	43.9	26.3	26.7	26.8	26.9
26.8	26.2	26.5	33.9	32.2	43.8	26.3	26.7	26.8	26.9
26.9	26.3	26.6	33.9	31.8	43.8	26.4	26.8	26.9	26.9
26.9	26.4	26.7	34.1	32	43.7	26.5	26.9	27	26.9
26.9	26.5	26.9	34.1	34.6	43.9	26.7	26.9	27.2	26.9
27.1	26.5	26.9	34.2	34.6	43.9	26.7	27	27.2	27.2
27.1	26.5	26.9	34.2	34.6	43.8	26.7	27	27.2	27.2
27.1	26.5	26.9	34.2	34.6	43.8	26.7	27	27.2	27.2
27.1	26.2	26.5	34.2	33.1	43.8	26.3	26.7	26.8	27.2

Table A13: Showing readings of Al_2O_3, 0.1% concentration at 45°C temperature when velocity of air was 6.00 m/sec and water flow rate was 25LPH.

T1	T2	T3	T4	T5	T6	T7	T8	T9	T10
24	27	35.5	34.7	27.4	44.1	27.2	27.6	27.7	27.9
23.5	27	34.2	34.9	27.3	44.1	27.1	27.5	27.6	27.9
23.7	26.9	34.4	34.9	27.3	43.9	27.1	27.5	27.6	27.9
23.5	27	34.4	35.1	27.3	43.9	27.2	27.6	27.7	27.9
24	27	34.4	35.2	27.3	43.9	27.2	27.6	27.7	27.9
24	27	34.4	35.2	27.5	43.9	27.2	27.8	27.9	27.9
24.2	27	33.5	35.2	27.4	43.9	27.2	27.7	27.8	27.9
24.2	27	33.5	35.2	27.4	43.9	27.2	27.7	27.8	27.9
24.2	27	35.5	35.2	27.4	43.9	27.2	27.6	27.7	27.9

Table A14: Showing readings of Al_2O_3, 0.2% concentration at 45°C temperature when velocity of air was 6.00 m/sec and water flow rate was 25LPH.

T1	T2	T3	T4	T5	T6	T7	T8	T9	T10
29.4	29	33.3	35.7	30	44.2	29.1	29.5	29.6	29.7
29.5	29	33.2	35.9	29.8	44.2	29.1	29.5	29.6	29.7
29.5	28.9	33.1	36.5	29.8	44.2	29.1	29.5	29.6	29.7
29.5	28.9	33.1	36.3	29.8	44.1	29.1	29.5	29.6	29.7
29	28.9	33.2	36.4	29.8	44.1	29.1	29.5	29.6	29.7
29	28.9	33.2	36.4	29.8	44	29.1	29.5	29.6	29.7
29.2	29	33.3	36.5	30	44	29.1	29.5	29.6	29.8
29.2	29	33.2	36.5	29.8	44	29.1	29.5	29.6	29.8
29.2	28.9	33.1	36.5	29.8	44	29.1	29.5	29.6	29.8

Table A15: Showing readings of Al_2O_3, 0.1% concentration at 50°C temperature when velocity of air was 6.00 m/sec and water flow rate was 25LPH

T1	T2	T3	T4	T5	T6	T7	T8	T9	T10
27.3	26.7	33.1	39.2	27	48.2	26.9	27.3	27.4	27.8
27.6	26.9	32.6	39.4	27.4	48.2	27.1	27.6	27.7	27.8
27.7	27.2	32	39.5	27.4	48.1	27.3	27.7	27.8	27.8
27.9	27.3	34.1	39.5	27.6	48.1	27.5	27.9	27.8	28
28	27.4	33.4	39.6	27.6	48	27.6	28	28.1	28.3
28	27.5	33.5	39.7	27.8	48	27.6	28	28.1	28.5
28.1	27.6	33.6	39.7	27.9	47.9	27.7	28.1	28.2	28.5
28.1	27.6	33.6	39.7	27.9	47.9	27.7	28.1	28.2	28.5
28.1	27.6	33.6	39.7	27.9	47.9	27.7	28.1	28.2	28.5

Table A16: Showing readings of Al_2O_3, 0.2% concentration at 50°C temperature when velocity of air was 6.00 m/sec and water flow rate was 25LPH

T1	T2	T3	T4	T5	T6	T7	T8	T9	T10
28.4	28.8	36.2	40.5	29.1	49.5	29	28.4	29.5	29.7
28.3	28.8	36.1	40.6	29.1	49.3	28.9	28.3	29.4	29.7
28.4	28.8	36.3	40.6	29.2	49.6	29	28.4	29.6	29.8
28.5	28.9	35.6	40.7	29.3	47.4	29.1	28.5	29.6	29.9
28.4	28.9	35.6	40.7	29.1	49.4	29	28.4	29.5	29.9
28.4	28.9	35.4	40.9	29.2	48.4	29	28.4	29.5	29.9
28.4	28.8	36.2	41	29.1	49.5	29	28.4	29.5	29.9
28.3	28.8	36.1	41	29.1	49.3	28.9	28.3	29.4	29.9
28.4	28.8	36.3	41	29.2	49.6	29	28.4	29.6	29.8